DNA repair mechanisms revisited By single molecule approaches

Judith Miné-Hattab

Habilitation à diriger des recherches

université PARIS-SACLAY

DNA repair mechanisms revisited By single molecule approaches

Habilitation à diriger des recherches de l'Université Paris-Saclay en Physique

présentée et soutenue à Paris, le June 16th 2022, par

Judith Miné-Hattab

Compositon du jury

Karine Dubrana DR, HDR, CEA, INSERM	Rapportrice
Timothee Lionnet Assistant Professeur, New York University	Rapporteur
Raphael Voituriez DR, HDR, Sorbonne Université, CNRS	Rapporteur
Nathalie Westbrook Prof, HDR, University Paris Saclay, CNRS	Examinatrice
Leonid Mirny Prof, MIT	Examinateur
Fabian Erdel HDR, University de Toulouse, CNRS	Examinateur

université
PARIS-SACLAY

Title : DNA repair mechanisms revisited by single molecule approaches.

Keywords : DNA repair, single molecule microscopy, nuclear organization.

Abstract : I am a biophysicist who is passionate about understanding how different kind of stresses can alter molecular organization and dynamics and the resulting consequences on cell functions. With an academic background in physics, through my doctoral and postdoctoral trainings, I have acquired expertise in a wide range of fields and techniques, including DNA repair, computational modeling, single molecule microscopy, genetics, molecular and cellular biology. I obtained my PhD at the Institut Curie in 2008 in the laboratory of Jean-Louis Viovy, where I studied the mechanical and torsional effects of repair proteins on DNA using *in vitro* single molecule approaches. I then joined the laboratory of Pr. Rodney Rothstein at Columbia University (New York) to investigate the choreography of DNA in living cells in response do DNA damage. Joining the laboratory of Xavier Darzacq at the Ecole Normale Supérieure de Paris, I learnt single molecule microscopy, an approach I am still using to address how nuclear organization is altered in response to various kinds of perturbations. In 2014 I joined the laboratory of Angela Taddei (Curie Institut) as a permanent researcher. I am starting a new team in 2022 at the Institut Biology Paris Seine in the Laboratory of Computational and Quantitative Biology.

Table of contents

Table des matières

Acknowledgement

It is with pleasure that I mention here all those who have contributed, followed or accompanied my work. First, I would like to thank all my mentors: Jean-Louis Viovy, Rodney Rothstein, Xavier Darzacq and Angela Taddei. Beside their different scientific expertise they brought me, I learnt from each of them a different way to think, to work and to manage a team. I hope to combine the best of each to continue my research during the next years.

Thank you to all my colleagues. It would be of course too long to cite each of them. Thank you to Marie Dutreix and Masayuki Takahashi, my collaborators in biology during my PhD, Giovanni Cappello, Chantal Prevost and Hideyuki Arata who accompanied me during my PhD work; thank you to Peter Thorpe, Robert Reid, Ivana Sunjevaric, Rebecca Bergess and Olga Marte who introduced me to yeast biology during my post-doctoral training; thank you to Ignacio Izeddin, Vincent Recamier and Bassam Hajj who initiated me to super resolution microscopy. I had the chance to work with great physicists, Thierry Mora, Aleksandra Walczak, Mathias Heltberg, Leonid Mirny: thank you for your interest and for all the discussions.

Thank you to all the members of the Taddei team and the PICT imagery plateform. My thanks go then to the persons who have accompanied this work very closely: the post-doctorants Cholé Guedj, Susmita Sridhar, Mathias Heltberg, Fabiola Garcia Fernandez; the students Siyu Liu, Manuela Baquero Perez, and the internship students Christel Michel, Gaizka Legoff and Fadma Lakhal.

Thank you to Emmanuel Hieaux and Alexandra du Bois, two music composers, for their contribution to the muse-IC project: discussing my experiments with them helped me to find the big picture in my work. A special thanks to Olga Markova for working with me several times to illustrate my work: during long discussions we had together. She made me realize that even when we believe we understand how things work, when it comes to drawing our ideas, many questions arise and new models emerge.

Thank you to my family, husband and kids. Most importantly, I would like to thank my parents: they showed me how to think on my own and how to realize projects that I love.

Presentation of the manuscript

My research aims to understand how our genome is altered by environmental stresses combining microscopy, genetics and bio-physical approaches. In particular, during my doctoral and post-doctoral trainings, I focused on the consequences of DNA damage, both at the molecular level by studying the mechanical and torsional effects induced by repair proteins on DNA *in vitro*, and at the nuclear level by quantifying the changed of chromatin dynamics upon double strand breaks. Through my doctoral and postdoctoral trainings, I have acquired experience in a wide range of fields and techniques, including DNA repair, molecular biology, single molecule microscopy and biophysical modelling. The experience and interest I gained over these years have been instrumental in defining the direction of my future research team.

The manuscript presents my research work from 2004 to 2022 including my doctoral, post-doctoral, current research and my future plans. Before presenting my work, the manuscript starts by an introduction on DNA repair. However, the goal of this introduction is not to provide an extensive review of the literature in the field of DNA repair, but rather to highlight some key points that inspire my research. From my doctoral work to my current research, I have used several model organisms: E. col, yeast and human cells. Since many fundamental questions have been addressed in E. coli, I will often refer to E. coli and compare mechanisms or models from different organisms throughout the manuscript.

CV

Judith Miné-Hattab, CR, CNRS

UMR3664 unit "Nuclear Dynamics",
Angela Taddei team “Compartmentalization and dynamics of nuclear functions”
Institut Curie, 26 Rue d’Ulm, 75005 Paris

Scientific interest : DNA repair, nuclear organization, super resolution microscopy, image analysis, diffusion of science

Academic positions

2022 (June) Junior Group Leader, Laboratory of Computational and Quantitative Biology, UMR7238, Institut de Biology Paris Seine.

2014 - 2022 CR CNRS/IC "Nuclear Dynamics", Angela Taddei team, Institut Curie, Paris, France.

Research Experience and Education

2012 - 2013 Post-doctoral fellow, Xavier Darzacq team, ENS, Paris, France.

2008 - 2012 Post-doctoral fellow, Rodney Rothstein, Columbia University Medical Center, New York, USA.

2004 - 2008 PhD, Jean-Louis Viovy team, UMR 168 Physico-Chimie, Institut Curie, Paris, France.

2001 - 2004 M2 “Solid States Physics and Condensed Matter”. Mention Bien.
« Magistère » in Fundamental Physics, Université Paris-Saclay. Mention Bien.

1999 - 2001 Deug MIAS (L1 & L2), Mathematics, Computer Sciences and Physics, Université Paris-Saclay. Mention Bien.

Funding (selection) and Prizes:

2022-2025: ATIP-Avenir “Nuclear architecture and dynamics of DNA repair in cells under compression” (300 k€)
2018-2022 : ANR generic “ RepairChrom ” – Partner (620 k€)
2018-2020 : Q-Life grant, « Physics of foci » - Coordinator (100 k€)
2017-2019 : PSLgrant « Aux frontières des Labex » Muse-IC project- Coordinator (65 k€)
2013-2017 : ANR Post-Doc return « DNA Dyna » - Coordinator (410 k€)
2010-2013 : Marie Curie IOF (International Outgoing Fellowship) (300 k€)
2008-2010 : EMBO Long-Term fellowship (180 k€)

2009: Prize from the Philippe Foundation to support French post-doc in USA
2008: Prize for young researchers from the Bettencourt Foundation
2008: Best inter-disciplinary PhD prize from the EADS

Publications

20 publications in peer-reviewed scientific journals ORCID ID : 0000-0001-9986-4092

Physical observables to determine the nature of membrane-less cellular sub-compartments.
Heltberg Mathias, Miné-Hattab Judith, Taddei Angela , Walczak Aleksandra M. , Mora Thierry.
eLife, 10:e69181, 2021

Single molecule microscopy reveals key physical features of repair foci in living cells
Judith Miné-Hattab*, Mathias Heltberg, Marie Villemeur, Chloé Guedj, Aleksandra M. Walczak, Thierry Mora, Maxime Dahan, Angela Taddei*, * co-corresponding authors.
eLife, 10: e60577, 2021.

Complex Chromatin Motions for DNA Repair
Judith Miné-Hattab***** & Irène Chiolo, * corresponding authors.
Frontiers in Genetics, 11: 800, 2020.

Physical principles and functional consequences of nuclear compartmentalization in budding yeast.
Judith Miné-Hattab, Angela Taddei.
Curr Opin Cell Biol. 2019.

Guidelines for DNA recombination and repair studies: Cellular assays of DNA repair pathways.
Klein et al.
Microb Cell, 2019.

When science and music meet
Garant Alberman, Jean-Marie Gagez, Judith Miné-Hattab
Medecine sciences: M/S, 35(11):881-885, 2019.

High-resolution visualization of H3 variants during replication reveals their controlled recycling" by Camille Clément, Guillermo Orsi, Alberto Gatto, Ekaterina Boyarchuk, Audrey Forest, Bassam Hajj, Judith Miné-Hattab, Mickaël Garnier, Zachary Gurard-Levin, Jean-Pierre Quivy, and Geneviève Almouzni.
Nature Communication, 9;9(1):3181, 2018.

Chromatin mobility upon DNA damage: a multi-scale story.
Judith Miné-Hattab*****, Xavier Darzacq, * corresponding author.
Medecine sciences: M/S, 2018.
Cover of the journal

Multi-scale tracking reveals scale-dependent chromatin dynamics after DNA damage.
Judith Miné-Hattab*[1], Vincent Recamier[1], Ignacio Izeddin, Rodney Rothstein*, Xavier Darzacq*.
[1]co-first author**.** *co-corresponding author.
Molecular Biology of the Cell**.** 28(23): 3323–3332. 2017.
Highlighted in MBoC.

Lamin A: a key protein in chromatin motion
Eldad Kepten, Judith Miné-Hattab*****, *corresponding author.
Medecine Sciences: M/S, 2017.

Lasker award 2015: spotlight on DNA repair.
Judith Miné-Hattab
Medecine Sciences: M/S, 32(1):123-4, 2016

DNA in motion during double-strand break repair.
Judith Miné-Hattab & Rodney Rothstein. Review.
Trends in Cell Biology, 23(11):529-36, 2013.

Increased chromosome mobility facilitates homology search during homologous. recombination**.**
Judith Miné-Hattab & Rodney Rothstein.
Nature Cell Biology 14(5), 510–517, 2012
Highlighted in:
Nature Reviews Molecular Cell Biology 13(5), 281, 2012.
Nature Cell Biology 14(5) , 448-450, 2012.

DNA repair : Finding the perfect match.
Judith Miné-Hattab* & Rodney Rothstein (*corresponding author).
Medecine Sciences: M/S 28(8-9), 714-716, 2012.
Cover of the journal.

Numerical modeling of homology search promoted by RecA or Rad51 proteins.
Judith Miné-Hattab, Geneviève Fleury, Chantal Prevost, Marie Dutreix, Jean-Louis Viovy.
Plos One 6(4):e14795, 2011.

Separation of time scales in the polymerization of nucleoprotein filaments.
Paolo Pierobon, Judith Miné-Hattab, Giovanni Cappello, Jean-Louis Viovy, Marco Cosentino Lagomarsino.
Physical Review E. 061904, 2010.

Direct observation of twisting steps during hRad51 polymerization on DNA.
Hideyuki Arata, Aurélie Dupont, Judith Miné-Hattab, Ludovic Disseau, Axelle Renodon-Cornière, Masayuki Takahashi, Jean-Louis Viovy, Giovanni Cappello.
PNAS 106(46), 2009.

Real-time measurements of the nucleation, growth and dissociation of single Rad51 DNA nucleoprotein filaments.
Judith Miné, Ludovic Disseau, Masayuki Takahashi, Giovanni Cappello, Marie Dutreix, Jean-Louis Viovy.
Nucleic Acids Research 35(21), 2007.

Mechanism of RecA-mediated homologous recombination revisited by single molecule nanomanipulation.
Renaud Fulconis*, Judith Miné*, Aurélien Bancaud, Marie Dutreix, and Jean-Viovy (* : co-first authors).
EMBO (18) 2006.

Nematic elastomer with aligned carbon nanotubes: New electromechanical actuators.
Sebastien Courty, Judith Miné, Ali Tajbakhsh, Eugene Terentjev.
Europhysics Letter 64(5), 2003.

Publication based on my work in Diffusion of sciences

The Sounds of science: biochemistry and cosmos inspire new music
Elie Dolgin
Nature **569**, 190-191, 2019

Book chapters:

Chromatin Dynamics upon DNA Damage
Judith Miné-Hattab & Xavier Darzacq
Book chapter, IntechOpen 2020

Gene targeting and Homologous Recombination in *Saccharomyces cerevisiae*
Judith Miné-Hattab & Rodney Rothstein
Springer Link, book entitled “Site-directed insertions of transgenes”, 2012

Mentoring

Supervision of M1/M2 students:

Christel Michel: M2, 4 months, 2016
Gaizka LeGoff: M1, 4 months, 2017
Manuela Baquero : M1, 5 months, 2018
Siyu Liu: M2, 6 months, 2018
Fadma Lakha: M2, 6 months, 2022

Co-Supervision of PhD students:

Manuela Baquero Perez (2019-2023)

Siyu Liu (2019-2022) 1 co-author publication in preparation

Supervision of post-doctorants:

Chloé Guedj: 2015-2016, 1 co-author publication
Susmita Sridhar: 2018-2020, 1 co-author publication in preparation
Fabiola Garcia Fernandez: May 2021 to present

Co-Supervision of engineer:

Marie Villemeur: october 2015-2020, 1 co-author publication, 2 co-authors publications in preparation.

Teaching

2015/2019 : L3 international semester, FdV program, Biophysics class (CRI), ~ 20h per year).

2004-2007 : L1/L2, optics at Paris Descartes University.

Science Dissemination

Organizer of the Muse-IC project: https://www.nature.com/articles/d41586-019-01422-0
https://www.mos.org/subspace/music-of-the-genome
http://bit.ly/projet-muse-ic

Member of the "ActinArt Association": https://www.actinart.com/index_fr.html

Science Communication (selection)

Selected speaker or invited speaker in international meetings (selection):
2022 : Epigenetics Course Institut Curie (Paris)
2021 : MiFoBio (Presqu'Ile de Giens, France)
2019 : Phase separation meeting (Paris)
2018: REsearch TUmors BIology ReTuBi Meeting (Lisbonne, Portugal)
2017: EMBO conference (2018), Gordon Research conference (Lucas, Italy)
2017: Epigenetics course Institut Curie (Paris)

Invitation to give seminars (selection):
2022: invited seminar and workshop at the France BioImaging AT (Paris)
2022: invited seminar at the MIT, Institute for Medical Engineering & Science, Boston, USA
2022: invited seminar at the Longy School of Music of Bard College, Cambridge, USA
2022: invited seminar at the UMR7216 – Paris Epigenetics, Paris
2022: invited seminar at the IBPS, Paris
2021: invited seminar at the UMR7196-U1154, Muséum national d'Histoire naturelle, Paris.

Other professional Activities

Editorial work as reviewer for: EMBO, elife, NAR, Cell report, Life Alliance, PNAS.

Grant Evaluations : National Science Centre, Poland, 2017, 2021
Evaluations for the IC3i International PhD Program in 2015, 2016, 2020.

Scientific animation and service to the community (selection):

2014 - 2022: Organization of the SiMoNa meetings (SIngle-MOlecule imaging of Nuclear Architecture) between UMR168, UMR3664, Institut Langevin.
2018 - 2022: Organization of the Nuclear Dynamics Series (monthly meetings)
2014 - 2018: Organization of the Yeast meetings (between CEA, the Institut Curie, IBPC…)

Career breaks

September 10th 2009 – January 10th 2010:	Maternity leave, 4 months.
February 2011 – September 2011:	Part-time work due to husband's illness, 7 months.
November 1st 2013 – March 1st 2010:	Maternity leave, 4 months.
November 15th 2018 – June 1st 2019:	Maternity leave, 6.5 months.

Introduction

1.1 DNA integrity and DNA repair

Throughout the life of a cell, its genome is constantly damaged by a variety of exogenous and endogenous agents. Among these agents are UV radiation or mutagenic agents. DNA can also be damaged during its own replication. It is estimated that the DNA of a human cell is subject to 50,000 to 500,000 lesions per day. Double Strand Breaks (DSB) represent only a very small fraction of the 50,000 to 500,000 DNA lesions that a cell must repair each day. In fact, it is estimated that a cell has only ~ 50 DSB to repair each day(Vilenchik and Knudson, 2003). In contrast to their low number, DSB are extremely toxic for the cell, as one of the chromosomes is cut in two parts. Healthy cells are able to repair DNA damages and preserve their genomic integrity. However, accumulation of DNA damages or improper repair can lead to mutations, loss of genetic information and cancer (Pastink et al., 2001). In higher eukaryotes, mutations in the DNA repair genes lead to diseases such as Werner, Bloom syndromes and cancer. Thus, DNA repair is an essential process for preserving genome integrity (Pastink et al., 2001).

Eukaryotic organisms use mainly two major mechanisms to repair DSBs: non-homologous end-joining and homologous recombination (HR). The relative use of these two pathways varies between species: homologous recombination predominates in yeast, whereas non-homologous end-joining contributes significantly to DSB repair in vertebrates. These two pathways also have different kinetics: NHEJ is a fast process which can be completed in approximately 30 minutes in human cells; whereas HR is much slower and takes 7 h or longer to complete. RH is a highly conserved process during evolution: the main steps and proteins of recombination have remained unchanged from bacteria to humans. My work focuses mainly on DSB repair by HR, both using *in vitro* and *in vivo* experimental approaches, using E. Coli, *Saccharomyces cerevisiae* yeast and human cells.

1.2 Homologous recombination: overview

In eukaryotes, HR is promoted by enzymes of the Rad52 epistasis group, including Rad51, Rad52, Rad54 and the Rad51 paralogues. These genes are highly conserved among eukaryotes, highlighting their importance for cell survival. When a DSB forms and HR is chosen to repair the break, HR occurs in several steps (Figure 1):

i) the 3’ ends of the DNA break are resected by nucleases to yield single-stranded DNA (ssDNA) tails on which Rad51 proteins polymerize. This Rad51-ssDNA complex is called the **nucleofilament.**

ii) The Rad51 nucleofilament has the capacity to search for homologous sequences throughout the entire genome if necessary, to locate a region of homology and then to promote strand invasion of the homologous duplex DNA. The search for a homologous double-stranded DNA (dsDNA) across the genome is considered a key step of homologous recombination. The **homology search** and the invasion of the nucleofilament into an intact homologous duplex DNA are stimulated by Rad52, Rad55/Rad57, Rdh54 and Rad54 proteins.

iii) Once homology is found, the stable assembly of the nucleofilament and homologous dsDNA forms a **synapsis**.

iv) Then, extensive **strand exchange** occurs between the nucleofilament and the dsDNA template within the synapsis, ultimately restoring genetic information disrupted at the DSB.

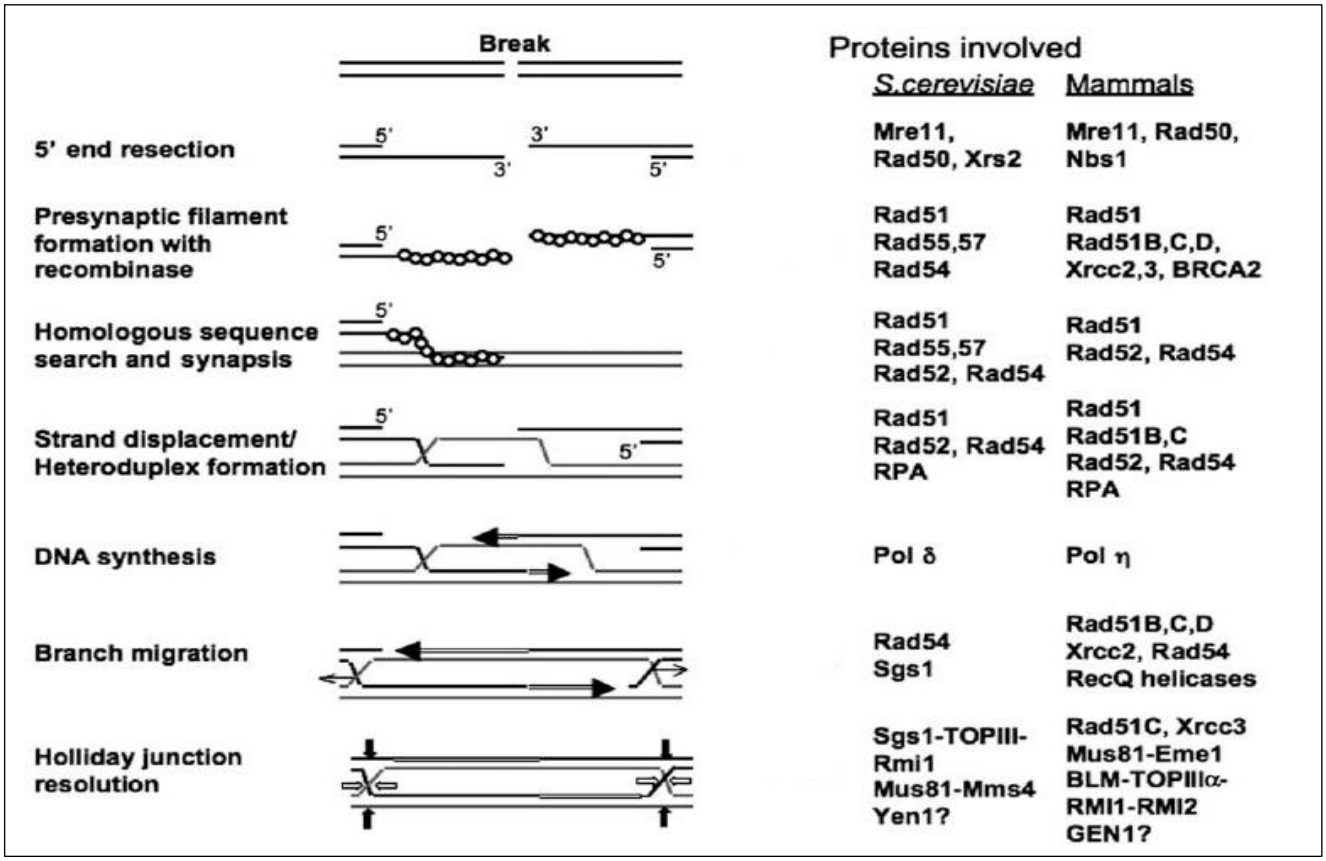

Figure 1 : View of homologous recombination and repair proteins associated in *S.cerevisiae* and mammals cells (Figure adapted from Hinz 2010).

1.3 RecA/Rad51 nucleofilament: structural and mechanical properties

One of the central protein of HR is RecA in E coli (Rad51 in yeast and mammals. During the polymerization step, RecA-like proteins form a right-handed helix around the ssDNA tail formed at the damaged site: inside this helix, DNA is extended in length by a factor of ~ 1.5 when compared to B-DNA (Dupaigne et al., 2008; Egelman, 2001; Hegner et al., 1999). The pitch of the nucleofilament is 90–13Å and the helix involves 6.4 - 6.5 monomers per helical turn (Conway et al., 2004; Egelman, 2001) (Figure 2). The precise values for RecA, ScRad51, hRad51, UvsX and RadA nucleofilaments are shown in Figure 3 (Egelman, 2001). Each hRad51 (human Rad51) monomer covers about three bases on ssDNA (Benson et al., 1994; Egelman, 2001). Interestingly, *in vitro,* RecA-like proteins can polymerize both on ssDNA and dsDNA: inside the helix formed on dsDNA, the dsDNA is also extended by a factor 1.5 but RecA-like proteins also change the DNA topology by unwinding dsDNA by ~15 ° per base pair. The affinity for ss *versus* dsDNA varies between species: for example, unlike RecA, hRad51 has a high affinity for dsDNA than for ssDNA *in vitro*. Finally, RecA/Rad51 can also form filaments in the absence of DNA, but the existence and biological relevance of such filaments remain unclear.

The persistence length quantifies the bending stiffness of a polymer. It represents the typical distance on which a macromolecule can be bent by Brownian forces. Naked dsDNA has a persistence length L_p of ~ 50 nm while ssDNA is extremely soft (L_p ~ 3 nm) (Bouchiat et al., 1999). One striking property of RecA/Rad51 nucleofilament is their stiffness. Using optical and magnetic tweezers, the persistence length of a RecA-ssDNA complex is estimated at ~ 400 nm when formed in the presence of ATP (~ 700 nm when formed with ATPγS) (Fulconis et al., 2006; Shivashankar et al., 1999). RecA

filaments are not static but rather form an equilibrium between polymerization and depolymerization. For RecA, the polymerization rate in the presence of ATP is ≈12 monomers/sec whereas the rate of depolymerization is ≈2 monomers/sec (Shivashankar et al., 1999).

At that point, little was known about the persistence length of hRad51 nucleofilaments, its polymerization/ depolymerization rate, and its polymerization mechanism. Thus, I focused on these questions during the first part of my PhD. Although hRad51 shares many structural and functional similarities with RecA and the general process of recombination is similar for both proteins, hRad51 differs significantly from RecA for certain biochemical characteristics. RecA has a very strong preference for nucleation on ssDNA (West, 2003) and ATP hydrolysis promotes its dissociation from ssDNA and dsDNA (Arenson et al., 1999) whereas hRad51 shows a preferential affinity for dsDNA (21), it has a very low ATPase activity (Tombline and Fishel, 2002) and ATP hydrolysis does not seem to correlate with hRad51 dissociation from dsDNA (Chi et al., 2006). Since efficient strand exchange requires preferential binding to ssDNA rather than dsDNA (7,17), this might explain hRad51's weaker strand-exchange activity *in vitro* when compared to RecA. It also suggests that one of the roles of the numerous other proteins involved in HR *in vivo* may be to favor the formation of hRad51 nucleofilaments on ssDNA over dsDNA ones. Such a role has been shown for Rad54 (24,25), Rad52 (26), Rad55 and Rad57 (27) and BRCA2 (28–30) in human. When I started my PhD, the polymerization of RecA has been extensively studies and several models of polymerization were proposed (Shivashankar et al., 1999; Turner, 2000). However, less was known about the kinetics of polymerization for hRad51.

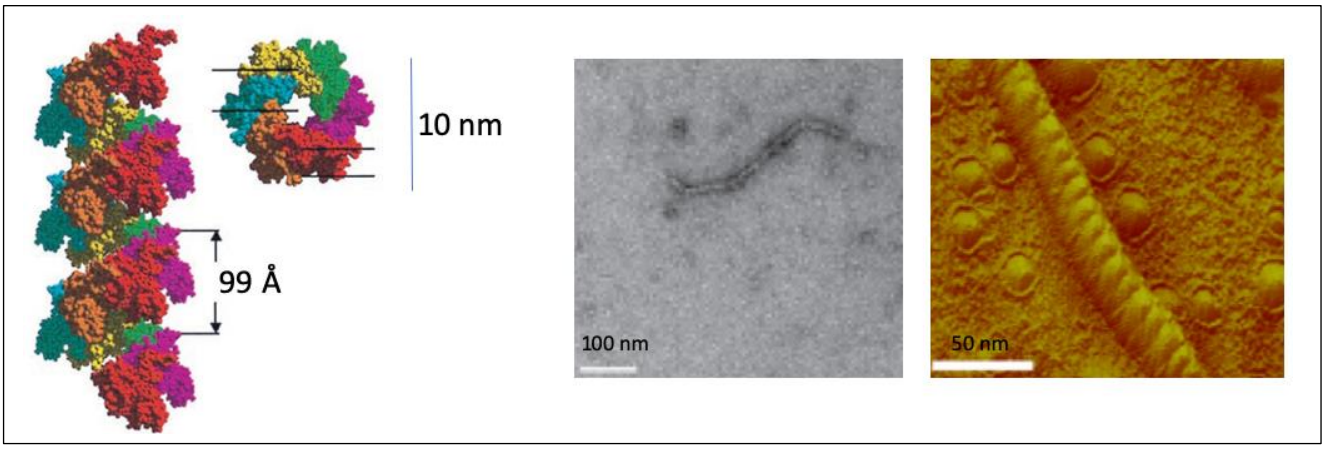

Figure 2 : RecA-like proteins form a helical structure around DNA. Left : structure of the human Rad51 (hRad51) filament from Hegner et al., 1999. Middle : ScRad51 (*S. cerevisiae*) nucleofilament on ssDNA (Liu et al 2011). Right : 3D view showing very clearly the right-handed helicoidal filament formed by ScRad51 on a dsDNA (AFM image), (Dupaigne *et al* 2008).

1.4 Homology search: models proposed in the literature

Once formed, the RecA/Rad51-ssDNA complex then searches for homologous sequences among neighboring dsDNA molecules. Homologous DNA strands are then exchanged when homology is found. Homology search remains a very enigmatic stage, with implications reaching beyond the range of DNA repair alone. HR can take place between sister chromatids, between alleles on homologous chromosomes of a diploid cell or between ectopic (non-allelic) homologous sequences. Homology search is surprisingly efficient. *In vitro*, a RecA nucleofilament is able to identify a homologous sequence among an excess of heterologous substrates 200,000 times greater in just 15 minutes (Sagi et al., 2006), a result recently confirmed in living E coli (Wiktor et al., 2021). In *S. cerevisiae* yeast, a single recipient locus and a single donor locus that share as little as 1.2 kb

of homology will find each other in the 15, 000 kb of condensed genome and engage in repair with 90% efficiency, no more than 2 hours after DSB formation (Aylon *et al*, 2003; Inbar *et al*, 2000).

Different hypotheses have been proposed to explain the high efficiency of homology search inside the genome. In the first hypothesis, the co-localization of the homologous sequences may precede the recombination-inducing lesion. This is often the case in sister chromatid recombination, which is the preferable DSB repair mechanism during G2 phase (Kadyk *et al*, 1992). However, in different settings, recombination occurs at high rates between homologous chromosomes and even between dispersed non-allelic homologous sequences (ectopic homology) (Haber *et al*, 1996; Aylon *et al*, 2003). Could these types of homologous sequences also be paired before the damage? Under this premise, and as the break point is typically not known in advance, we would have to assume that the position of homologous sequences is an innate general characteristic of the special organization of the genome and is used in the event of DNA damage. Although there is some evidence for this pairing in Drosophila, there is no evidence to support this idea in yeast or mammalian cells. By contrast, in another hypothesis, we assume that there is no pairing prior to the DSB. In this case, the broken molecule must somehow swiftly scan the immense and condensed genome to find a homologous sequence. Several models have been proposed to understand how homology search work in living cells.

The null model for homology search

The null model is an over-simplification of the situation upon DSB in which each base can be tested independently (Barzel and Kupiec, 2008). Let's examine the null model in a budding yeast nucleus. *A priori*, each of the 3×10^7 base pair of a G2 haploid *S. cerevisiae* genome might mark the beginning of the desired homologous segment. If we take the homology assessments of the candidates to be sequential, equal and independent, then it would take 3×10^7 trials on average for a recipient to find its appropriate donor. As a homology search in each cell takes between 1 hour and 2 hours, the time from the beginning of one trial to the beginning of the next should be approximately 2.5×10^{-4} seconds to allow for the null model ($2.5\times10^{-4} \cdot 3\times107 = 7{,}500$ seconds = 125 minutes). As a reference, it takes more than 40 times as long ($>10^{-2}$ seconds) for a DNA polymerase to add a single nucleotide to a growing DNA chain. Moreover, simply getting near a candidate sequence is probably insufficient to assess homology and be perfectly aligned. Overall, the "null model" has been rapidly rejected (Barzel and Kupiec, 2008).

Is a 1.5 elongation an advantage for homology search and strand exchange ?

During polymerization and homology search, the single strand end of the DSB is stiffened and stretched by the RecA/Rad51 proteins: this complex is then efficient to find a homologous sequence among concurrent sequences at large excess. We understand the interest of stretching the single strand end of the DSB to make homology search: indeed, in the absence of RecA and SSB (Rad51 and RPA in eukaryotes), the single-stranded end would form a ball of ssDNA totally inapt for homology search. However, why RecA/Rad51 stretch dsDNA by a factor 1.5 and unwind it by 15° compared to its native form?

Interestingly, all RecA-like proteins stretch DNA by the same factor and unwind dsDNA with a very similar angle (Egelman, 2001) (Figure 3). The fact that these properties have been well conserved during evolution is probably not a coincidence: DNA elongation by RecA/Rad51 monomers might play a role in the homologous recombination process, maybe favoring homology search and/or strand exchange.

An earlier study showed that RecA/Rad51 proteins bound to stretched dsDNA more rapidly than to B-DNA, leading the authors to suggest that the DNA conformation amenable to RecA binding

arises naturally from thermal fluctuations (Leger et al., 1998). In this interpretation, RecA-like proteins are merely stabilizing a pre-existing conformation of potential dsDNA templates that are a crucial intermediate in recombination between two DNA molecules.

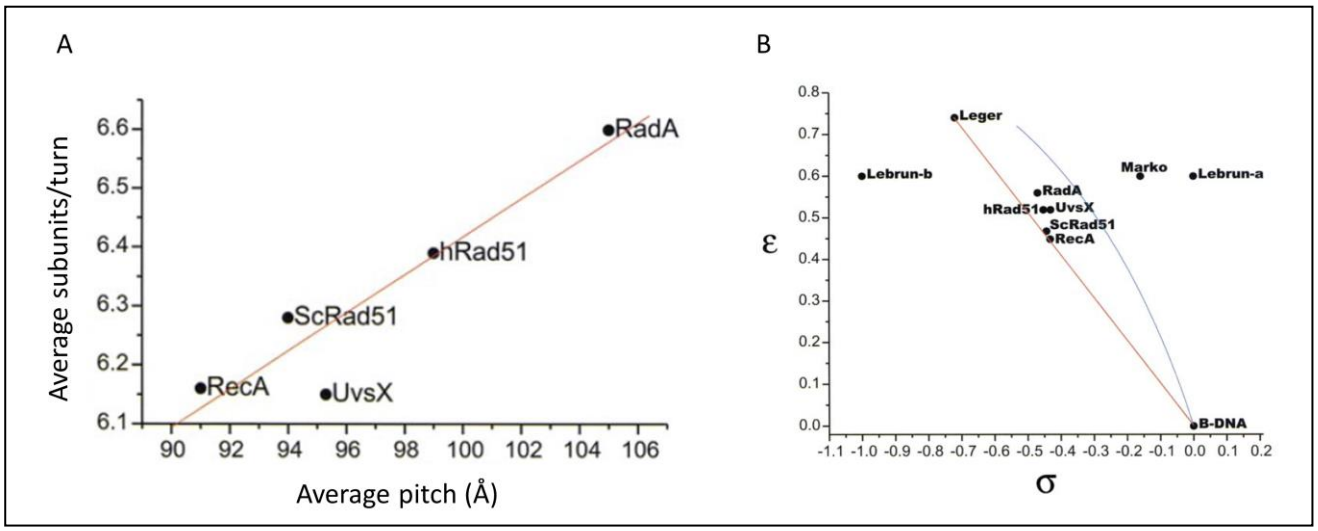

Figure 3 : RecA-like nucleofilaments through evolution. A) : Mean number of monomers per helical turn as a function of the helical pitch for E.coli, ScRad51, hRad51, UvsX et RadA. B) : Relative unwinding of dsDNA (σ) as a function of the relative extension ε. $\sigma = (\Delta\theta/\Delta\theta_0) - 1$ and $\varepsilon = (\Delta z/\Delta z_0) - 1$). $\Delta\theta_0$ is the twist of B-form DNA per basepairs (~34,5°) and et $\Delta\theta_0$ is the helical pitch of the B-form DNA (3.4°A).

The "breathing model":

Following these ideas, in a minimal model, Dorfman *et al.* proposed that homology search occurs in 2 steps. The first step deals with the approach of the target sequence in close vicinity of the homologous probe. In a second step, one must consider the more local mechanism leading to actual initiation of recognition and exact pairing (Dutreix et al., 2003). The first step involves diffusion to any nonspecific binding site on the DNA following the Rouse model (Andrews, 2014), while the second step comprises a series of translocation events that can also be driven by thermal fluctuations from the B to the S-form of DNA. Hence, thermal fluctuations could be a key role to enabling the initiation of local homologous recognition. To see if this hypothesis makes sense, Dutreix *et al.* roughly estimated the search time one would expect on the basis of this mechanism (Dutreix et al., 2003). They estimated that the large-scale search, allowing the nucleofilament to come to the vicinity of a homologous sequence, would take 10 second in a E. coli and the complete search time, including the exact pairing by breathing of the dsDNA would take 500 seconds, assuming a 1 kbases nucleofilament.

Using this model, Dorfman *et al.* proposed that global homology search driven by Rouse diffusion occurs at large scale ($d > l_{kuhn} = 100$ nm) while local homology search driven by thermal fluctuations occurs at $d < l_{kuhn} = 100$ nm. A They derived a formula giving the search time $< t >$ (Dorfman et al., 2004)**:**

$$< t > \approx \tau\left(\frac{R}{l_k}\right)\left[\frac{e^{-V/k_BT} + \alpha(1-e^{-V/k_BT})}{2\epsilon n_{bp\sqrt{k}}}\right],$$

where τ is the time of a contact, R is the characteristic size of the volume inside which homology search occurs, l_K is the Kuhn segment (2 times the persistence length), V is the attractif potential between DNA and RecA nucleofilament, α is the fraction of sites occupies by the filament, ε =

$k_{B\rightarrow S}/k_{S\rightarrow B}$ is the kinetics constants from B to S-phase DNA and n_{tot} is the total number of DNA bases.

Using this formula, Dorfman *et al.* found a recognition time of 500 seconds, equal to the experimental recognition time, only if they assume that the recognition starts with a seed of 3 basepairs. This parameter is thus central for their model: if we lower this parameter from 3 to 2, the typical recognition time becomes 5 seconds, if we increase it to 4, it becomes 18.5 hours ! Thus, the model works only when the recognition is initiated on 3 bases.

Life time of a synapsis during homology search

Using FRET *in vitro*, Sagi *et al.* estimated the lifetime of a synapsis during homology search (Sagi et al., 2006). For this, they incubated a RecA-ssDNA with dsDNA molecules with partially homologous sequences. These dsDNA molecules act as competitors during homology search with respect to a labeled homologous dsDNA. They measured the characteristic time of exchange for different levels of homologies. This characteristic time τ is the sum of contributions due to: (i) the formation of the RecA-ssDNA nucleofilament, (ii) the diffusion time of the nucleofilament to find a partner dsDNA, (iii) the synapse lifetime, (iv) and finally the time necessary for the strand exchange. In the absence of dsDNA competitors, the characteristic time τ is 1.9 ± 0.3 minutes, whereas it reaches 4.7 ± 0.3 in presence of fully heterologous dsDNA. The difference in τ between an experience without dsDNA competitors and in the presence of totally heterologous competitors gives access to the life time of a synapse. These experiments conclude that the lifetime of a synapsis is 10 to 15 seconds. Of note, it is possible that only synapsis with sufficiently long lifetime are detected experimentally.

As we have seen before, the total time of homology recognition is estimated at 500 seconds (Dutreix et al., 2003). Taken a lifetime of a synapsis of 10 seconds, it means that a RecA nucleofilament would form about 50 synapses before finding a homology.

1.5 Molecular diffusion

The mode of diffusion of a locus reveals aspects of how it explores nuclear space, how it deals with the obstacles it encounters, and how its movement relates to the organized structure of the nucleus. Thanks to the development of advanced microscopy techniques during the last 10 years, it has become possible to measure and quantify chromatin mobility in living cells. In the following section, I explain the approach I used to study molecular diffusion in the context of DNA repair.

The MSD approach:

The most common method to measure chromatin mobility consists of inserting a fluorescently tagged array at a given genomic locus and measuring its position through time. To tag a locus, repeated bacterial sequences, such as Lac-Operator (*lacO*) or Tet-Operator (*tetO*) arrays are inserted in the genome (Klein et al., 2019). These arrays are bound by Tet-Repressor (TetR) and Lac-repressor protein (LacI), which are fused to fluorescent proteins. The genomic locus is visible as a fluorescent spot by wide field microscopy and can be tracked over time. It should be noted that, in some cases, tightly bound LacI and TetR repressors can create fragile sites or constitute a barrier of unknown penetrability to DNA processing enzymes (Jacome and Fernandez-Capetillo, 2011). To overcome these barriers, variants of LacI, such as the LacI** mutants (Dubarry et al., 2011), have been used as alternatives to bypass any possible bias. Another tagging method, consisting of the ParBINT DNA labelling system, has also been developed to fluorescently mark genomic loci (Saad et al., 2014).

Types of diffusion:

Once the experimental trajectory of a locus is determined, its diffusion properties are quantified by calculating its mean-square displacement (MSD) (Saxton and Jacobson, 1997). The MSD curve represents the amount of space a locus explores in the nucleus, and its shape reveals the nature of chromatin motion (Figure 4). The time-averaged MSD of a single trajectory is calculated using the following equation:

$$\boldsymbol{MSD(n \cdot \Delta t) = \frac{1}{N-n}\sum_{i=1}^{N-n}[(x_{i+n} - x_i)^2 + (y_{i+n} - y_i)^2 + (z_{i+n} - z_i)^2],}$$

where N is the number of points in the trajectory, (*x*, *y*, *z*) the coordinates of the locus in 3-dimensions. In practice, chromatin dynamics is measured in several nuclei averaged MSD curves among several cells (time-ensemble-averaged MSD) are calculated. To understand the type of motion a chromatin locus undergoes, MSD curves are fitted using the different models presented below (illustrated in Figure 4).

Brownian diffusion:
When a particle freely diffuses, its MSD curve is linear with time and its motion is called "Brownian". In this case, the MSD follows:

$$MSD\ (\Delta \cdot t) = 2 \cdot d \cdot D \cdot \Delta t$$

where *d* is the dimension of the movement, *D* is the diffusion coefficient of the locus, and *Δt* is the time interval use during the experiment to track chromatin.

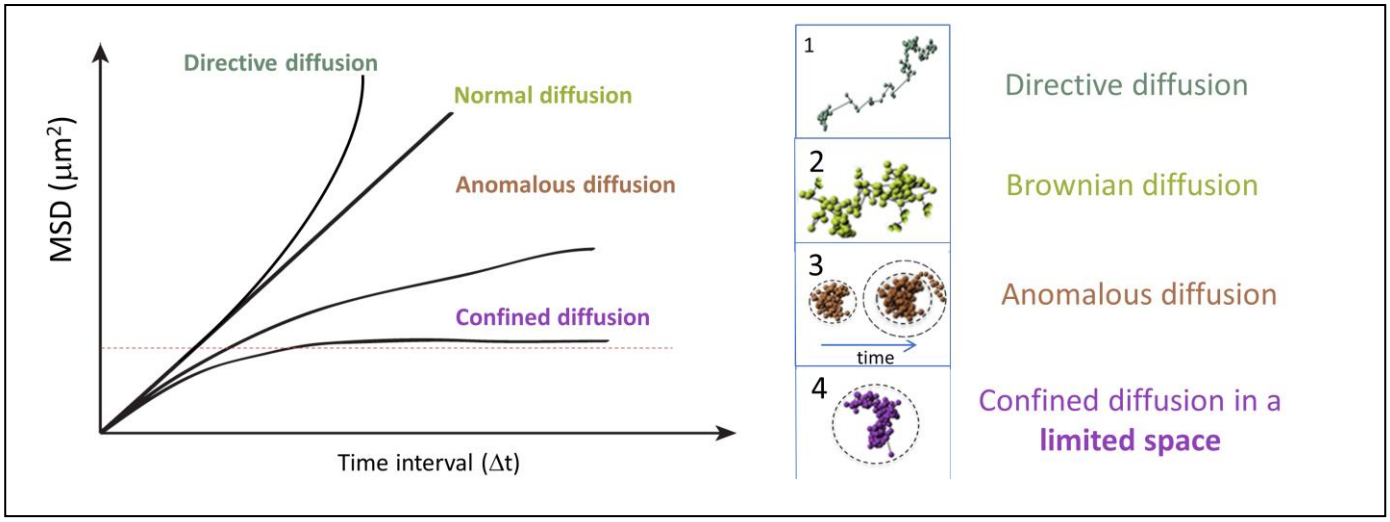

Figure 4 : Models of molecular diffusion. Left, theoretical Mean Square Displacement (MSD) curves for directive, Brownian, anomalous, confined and directive diffusion. Right: corresponding typical trajectories for each mode of diffusion (Klein et al, 2019).

Sub-diffusive diffusion:
In living cells, DNA motion is often slower than Brownian diffusion and is called "sub-diffusive diffusion" (Barkai et al., 2012). Two types of sub-diffusive diffusion have been described: confined sub-diffusion and anomalous sub-diffusion.

Confined sub-diffusion:
When a chromosomal locus stays confined inside a sub-volume of the nucleus, its motion is called

confined sub-diffusion. The MSD exhibits a plateau (Marshall *et al.*, 1997) and follows the equation:

$$MSD = R_{\infty}^2(1 - e^{-2 \cdot d \cdot D \cdot t / R_{\infty}^2})$$

where R_∞ is the measured plateau of the MSD, and *D* is the diffusion coefficient of the locus.
The confinement radius (*Rc*) of the motion is given by the relation: $R_c = R_\infty \sqrt{(d+2)/d}$, where *d* is the dimension of the motion. The MSD curve starts to bend at time $t_c = R_\infty^2/(2 \cdot d \cdot D)$, reprensenting the characteristic, equilibration time, after which the effect of boundaries appears.

Anomalous sub-diffusion:
When the force or structure that restricts the motion is not a simple confinement but is modulated in time and space with scaling properties, the motion is called *anomalous sub-diffusion* (Barkai et al., 2012; Metzler et al., 2014). In this case, sub-diffusive loci are constrained, but, unlike confined loci, they can diffuse without boundary and thus reach further targets if given enough time. For sub-diffusive motion, the MSD exhibits a power law,

$$MSD = A \cdot t^{\alpha}$$

where α, the anomalous exponent, is smaller than 1.
The anomalous exponent α is linked to the degree of recurrence of DNA exploration, that is, the number of times a DNA locus reiteratively scans neighboring regions before reaching a distant position (Ben-Avraham, 2000). When α is small, the locus explores recurrently the same environment for a long time, while a large α indicates that the locus is able to explore new environments often. The anomalous diffusion coefficient A represents the amplitude of DNA motion; it is proportional to the diffusion coefficient only in the case of normal diffusion (when α = 1), which is rarely observed in biological systems (Barkai *et al.*, 2012).

Experimental MSD curves are affected by the noise. The localization accuracy can be affected by 2 sources of noise: i) the error in the determination of the accurate particle position due to convolution with the point spread function (PSF) and the finite number of photons, ii) the error due to the movement of the particle during the camera acquisition. This error is more important with higher exposure times and is sometimes referred to as "motion blur". As a consequence, experimental MSD have an additional term which has been calculated analytically in the case of Brownian motion (Michalet, 2011) and anomalous motion (Miné-Hattab et al., 2017).

After discussing all this points, I will present my past and present research work as well as my future plans. I chose to highlight some of the results with more details and to refer to the publications for other projects.

1. Doctoral research

1.1 Experimental approach: magnetic tweezers

Numerous efforts have been devoted in the last 20 years to the unraveling of the mechanisms of HR, from genetics, biochemistry in bulk to single molecule approaches and theoretical models. During my PhD, we choose to study the different steps of HR using magnetic tweezers. Indeed, since RecA/Rad51 proteins act both on the elongation and the torsion of dsDNA, magnetic tweezers is a relevant experimental approach because it is the only technique allowing us to control both the force and the torsion of a single DNA molecule while measuring its extension (Figure 5).

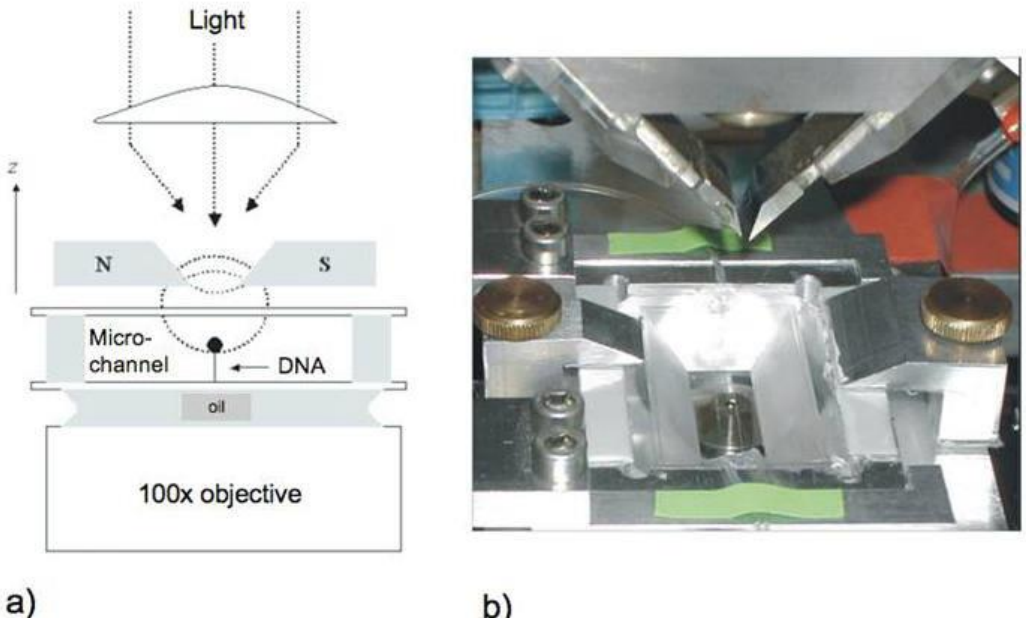

Figure 5: The magnetic tweezers set-up. A single DNA molecule is attached by one end to the bottom surface of a microfluidic flow cell and by the other end to a magnetic bead. A pair of magnets placed above the cell creates a magnetic field with a horizontal direction and a strong vertical gradient that pulls the bead upwards. By moving the magnets in the z dimension, one can tune the force stretching the molecule in the range of 0.001-15pN with a precision of 10%. The extension of the DNA molecule is given by the distance between the bead and the glass surface, measured by real-time analysis of the bead's image recorded at 120 Hz through a 100X objective, with accuracy typically better than 5 nm. By rotating the magnets, one can control the DNA topology.

1.2 Mechanical properties of human Rad51 nucleofilaments

Using magnetic tweezers, we first observed the polymerization mechanisms of human Rad51 (hRad51) both on ssDNA and nicked dsDNA (dsDNA containing a break on one of its strand and thus not constrained on torsion). The results presented here are described in details in (Miné et al., 2007, p. 51; Pierobon et al., 2010).

Like the RecA protein, we showed that hRad51 polymerization is initiated by the formation of a "nucleation seed" formed by 5.5 ± 1.5 monomers. Interestingly, the size of the nucleation seed is very close to the helical pitch of the Rad51 filament (6.4 monomers per helical turn) and similar

for RecA nucleation (Shivashankar et al., 1999). We proposed that, both for RecA and hRad51, the nucleation corresponds to the formation of a helical turn, and growth is facilitated once the first helical turn is formed (Miné et al., 2007; Pierobon et al., 2010).

However, the mechanisms of polymerization are radically different from RecA to hRad51. The polymerization kinetics of hRad51 exhibit different regimes depending on the protein concentration. At low protein concentration, the polymerization is very cooperative (reaction limited by the nucleation) whereas at high protein concentrations, it is not very cooperative, starting from multiple nucleation sites (growth-limited reaction). A Rad51 monomer binds 3 nucleotides: thus polymerization from multiple nucleation sites can often lead to 1 or 2 nucleotides gaps in the filament. The discontinuity of hRad51 filament and the formation of patchy hRad51 nucleofilaments strongly different from RecA (Shivashankar et al., 1999) and has been confirmed in other *in vitro* studies (Modesti et al., 2007). Importantly, hRad51 polymerization is extremely sensitive to hRad51 concentration: thus, over-expressing Rad51, for example by introducing a tagged Rad51 on a plasmid *in vivo* often give aberrant observations.

Second, we have shown that the initial rate of polymerization is faster on ssDNA than on dsDNA, but depolymerization from ssDNA is 150 times faster than that from dsDNA. We conclude that the apparent higher affinity of hRad51 for dsDNA observed in solution is in fact only due to a very low hRad51 depolymerization from dsDNA. These results suggest the existence of another mechanism probably provided by the partner proteins of hRad51 such as Rad54 or Rdh54.

To understand the polymerization mechanisms of hRad51, I proposed a simple model and fit the experimental polymerization curves (extension *versus* time). In the case of nicked dsDNA, we found that hRad51 depolymerization can be neglected:

$$\frac{dn}{dt} = k_a(N - n(t)), \qquad n(t) = N(1 - e^{-k_a t})$$

where N is the total number of hRad51 monomers that can polymerize on dsDNA

k_a is the hRad51 binding rate constant to dsDNA in s^{-1}.

Thus, the extension of the Rad4 complex is obtained by : $l(t) = l_i + (l_f - l_i)(1 - e^{-k_a t})$, where l_i is the initial extension of the dsDNA before the injection of hRad51 due to the force exerted by the tweezers and l_f is the final extension of the hRad51 filament measured at the end of polymerization. By fitting the experimental curves of hRad51 polymerization for different forces applied on dsDNA, we extracted the binding rate k_a and found that k_a increases exponentially with this force. According to the Arrhenius law, we expect : $k_a = Ae^{-E_a/k_B T}$, where E_a is the activation energy for hRad51 protein binding. This exponential decrease suggests that E_a decreases linearly with the stretching force. By measuring the binding rate ka for different forces applied on DNA, and using the Arrhenius low, we found that the activation energy of a hRad51 is ΔEa / RT ~ 0,21 pN−1 .

hRad51 polymerisation on ssDNA strongly differs from dsDNA and depolymerization had to be taken into account to fit the experimental curves:

$$\frac{dn}{dt} = k_a\big(N - n(t)\big) - k_d n(t)$$

where k_a is the hRad51 binding rate constant, k_d is the dissociation rate constant and N is the maximum number of hRad51 monomers that can polymerize on a ssDNA molecule.

Which leads to $n(t) = N\frac{k_a}{k_a + k_d}(1 - e^{-(k_a + k_d)t}$. The polymerization curves for hRad51 on ssDNA were well fitted with the following equation: $l(t) = n(t) * 3 * 1.5 * d_0 + l_i * \frac{N_{tot} - n(t)}{N_{tot}}$.

Finally, the persistence length of Rad51 nucleofilaments was measured by fitting their

experimental force *versus* length behavior to the worm-like chain (WLC) model (Bouchiat et al., 1999) in a large range of forces (typically from 10^{-3} to 10 pN) after full completion of the polymerization. The nucleofilament being not totally homogeneous, the persistence length extracted from the WLC model is only an average value, and it will be called effective persistence length in the following. We obtained a persistence length for the hRad51 of ~360 nm and 390 nm for hRad5 nucleofilaments formed on ssDNA and dsDNA respectively. Table 1 presents a summary of the mechanical properties of hRad51 nucleofilaments (see (Miné et al., 2007) for more details).

	hRad51	
	ssDNA	DsDNA
Persistence length with ATP (WLC)	360 ± 30 nm	390 ± 150 nm
Persistence length with ATPγS (WLC)	670 ± 30 nm	270 ± 80 nm
Average percent coverage in the presence of ATP	88 ± 2% (3 µM hRad51, 6 pN)	82 ± 2% (200 nM hRad51, 6 pN)
Average percent coverage in the presence of AMP-PNP	72 ± 5% (3 µM hRad51, 6 pN)	45 ± 16% (200 nM hRad51, 6 pN)
Average percent coverage in the presence of ATPγS	72 ± 3% (3 µM hRad51, 6 pN)	35 ± 4% (200 nM hRad51, 6 pN)
Initial polymerization velocity in the presence of ATP ($nm\,s^{-1}$ and $monomers\,min^{-1}$)	80 ± 10 $nm\,s^{-1}$ 8000 ± 1000 $monomers\,min^{-1}$ (3 µM hRad51, 6 pN)	7.8 ± 0.2 $nm\,s^{-1}$ 840 ± 20 $monomers\,min^{-1}$ (200 nM hRad51, 6pN)
Depolymerization velocity in the presence of ATP	450 $monomers\,min^{-1}$ (6 pN)	3 $monomers\,min^{-1}$ (6 pN)
Cooperativity during polymerization, with ATP (number of monomers involved in a nucleus)	–	5.5 ± 1.5

Table 1: Summary of the data on hRad51 nucleofilament assembly/disassembly and mechanical properties.

1.3 Strand exchange: the "zip" model inspired by single molecule experiments

I then focused on the strand exchange reaction between a RecA nucleofilament and a homologous dsDNA *in vitro* (Figure 6, left panel). To observe the mechanisms behavior of molecules during strand exchange at the single molecule level, we designed an experiment in which a ssDNA covered by RecA is held in the tweezers in the presence of homologous dsDNA molecules (Figure 6A). After 1h of incubation, we used force *versus* length curves as a readout to characterize the percentage of ssDNA *versus* dsDNA in the heteroduplex molecule formed (Figure 6B, left panel). The percentage of ssDNA and dsDNA in the hybrid molecule formed after strand exchange in the tweezers is calculated using a linear combination of each: $L_{hybrid}(F) = a \cdot L_{db}(F) + b \cdot L_{ss}(F)$, where L(F) is the length as a function of the force applied by the tweezers, a and b are the percentages of ds and ssDNA respectively. We found that strand exchange was performed in 75% of the molecule help in the tweezers (Figure 6B, left panel). Monitoring the length of the nucleofilament held in the tweezers during the strand exchange reaction revealed that its length decreased to about 4.5 µm, close to the length of a naked dsDNA with the same number of bp under the same force (Figure 6B, right panel). This key observation strongly suggests that RecA neither remains nor repolymerizes extensively on the exchanged duplex, otherwise the length of the molecule held in the tweezers would remain constant.

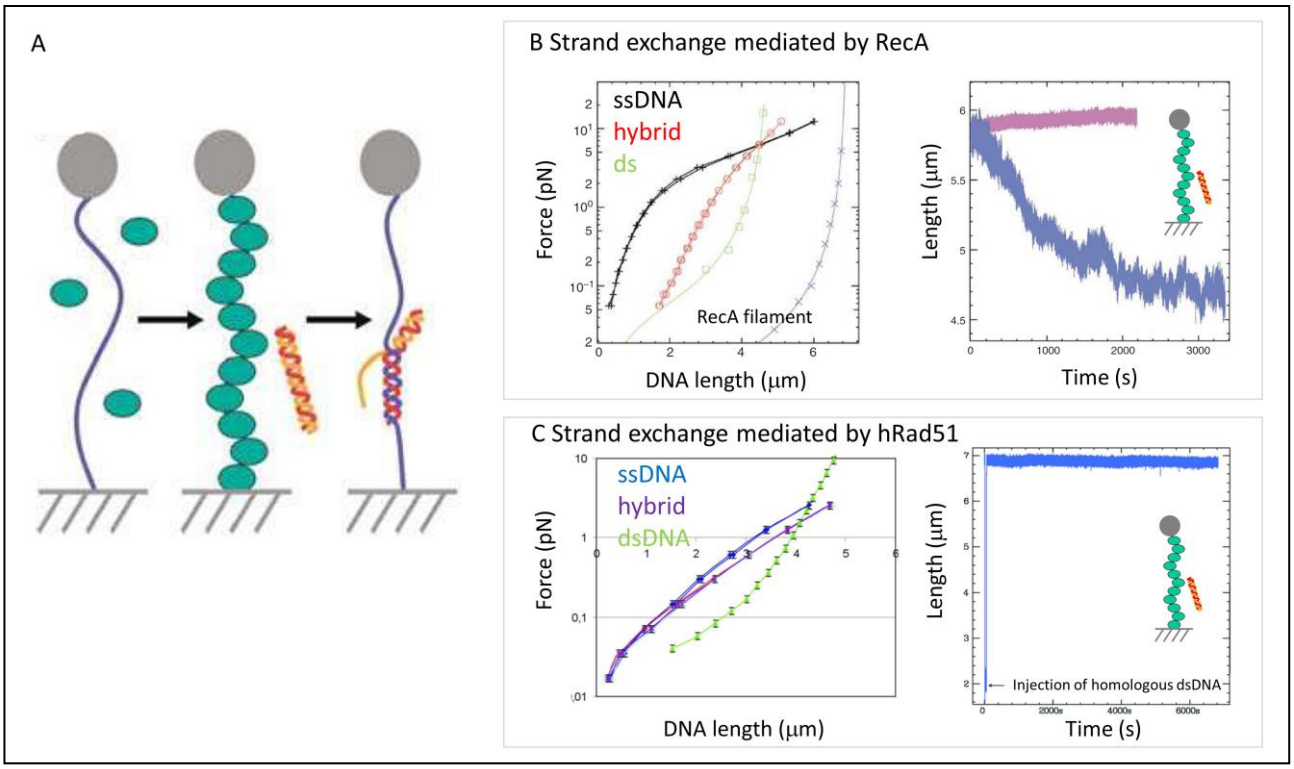

Figure 6 : Strand exchange inside magnetic tweezers. A: a ssDNA (14 kbases) is held in the tweezers and covered by RecA or Rad51 proteins. Homologous dsDNA molecules are incubated (several sizes of dsDNA were tested). B: left: Force *versus* extension curves measured at the beginning of the experiment on the ssDNA held in the tweezer (black), after incubation with RecA proteins (purple), and at the end of the strand exchange reaction (red, hybrid molecule). The force/extension curve of a dsDNA is shown as a reference (green). Right: length of the molecule held in the tweezers during the incubation with homologous dsDNA (bleu curve) or heterologous dsDNA used as a control (purple). C: Similar experiment when strand exchange is mediated by hRad51 instead or RecA.

This observation as well as complementary experiments led us to propose a new model for strand exchange. Unlike the common view of strand exchange where the RecA nucleofilament is aligned with its homologue along several thousands of bases, our results at the single molecule level revealed that the region of strand exchange (named synapsis) is extremely short (less than 1 kbase). To perform strand exchange over several thousand of bases, the synapsis moves like a “zipper” inside which strand exchange occurs (Fulconis et al., 2006) (Figure 7).

Performing similar experiments of strand exchange *in vitro* with hRad51, I found that the strand exchange reaction mediated by hRad51 alone didn’t reach a high efficiency (30% of strand exchange *versus* 75% for a reaction mediated by RecA) (Figure (6C, left panel). In addition, hRad51 was not able to depolymerize from the heteroduplex formed after strand exchange, since the length of the molecule held in the tweezers remains constant during the strand exchange reaction (Figure 6C, right panel). Our results show that the “zip model” could not describe strand exchange mediated by hRad51 alone. It would be interesting to test reproduce similar experiments in the presence of partners proteins of hRad51, such as Rad54. Unfortunately, I was not able to obtain purified Rad54 in the time frame of my PhD to validate the “zip model” in human.

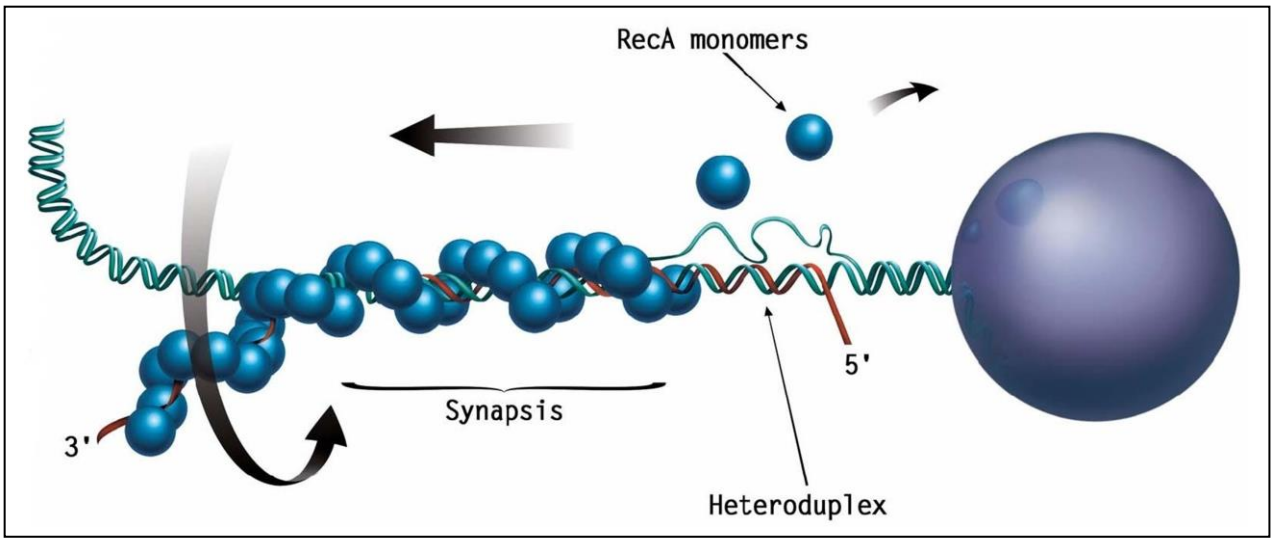

Figure 7 : the "zip" model: a new model of RecA-mediated strand exchange inspired by *in vitro* single molecule experiments. DsDNA is invaded by spooling (black arrow) on a synapsis progressing 5'–3' on the ssDNA nucleofilament. Depolymerization of RecA at the rear of the synapsis releases naked dsDNA and an exchanged ssDNA. We estimated that the synapsis is very short (less than 1kbases).

1.4 Tomotweezers: combining magnetic tweezers and fluoscence

During my PhD, I also had also the chance to design and build a new set-up combining magnetic tweezers and fluorescence measurements: the tomo-tweezers (Disseau et al., 2009) (Figure 8). Magnetic tweezers and fluorescence microscopy are among the most useful single-molecule approaches and the combination of these two techniques in a single assay offers a powerful tool for studying molecular systems. The tomo-tweezers set-up allows us to visualize the interactions between tagged protein or a DNA molecule by single-molecule fluorescence while simultaneously measuring mechanical and topological transitions with the tweezers. As a proof of concept, I applied this technique to visualize the interaction between a dsDNA and RecA nucleofilaments marked at one extremity by a quantum-dot.

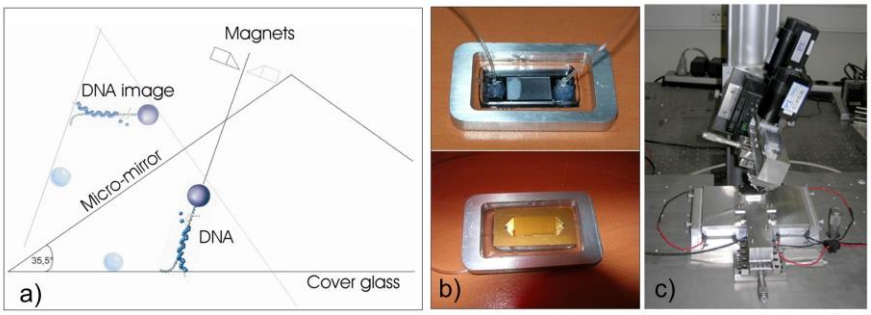

Figure 8: Principle of the tomo-tweezers setup. A) single double-stranded DNA molecule is held in magnetic tweezers inside a micro-channel fluidic device containing a series of micro-mirrors.

The DNA molecule is held in the tweezers with an angle of 19° in such a way that its image by the micro-mirror is horizontal allowing the observation of the entire molecule. b): pictures of the micro-mirrors used in the tomo-tweezers. B) Picture of the micro-fluidic chamber containing micro mirrors. C) Picture of the tomo-tweezers set-up I built during my PhD in Jean-Louis Viovy's laboratory.

During my PhD, I also contributed to several other studies which I won't detail here, exploring local homology search using Monte Carlo simulations (Miné-Hattab et al., 2011), the torsion induced on dsDNA by hRad51 (Arata et al., n.d.) and the theory of hRad51 polymerization (Pierobon et al., 2010).

From *in vitro* to *in vivo* biophysics:

To fully understand the complex mechanisms of DNA repair by recombination, it is necessary to develop multi-disciplinary research approaches, from molecular to cellular scale and to reconcile the results obtained by single molecule experiments, biochemistry and cell biology approaches. After my PhD, I decided to move to a biology laboratory to study chromosome dynamics in the context of DNA repair. I propose to join the Rodney Rothstein laboratory at Columbia University, New York, which is among the most famous in the field of DNA repair. There, I investigated how DNA motion is affected in response to DSBs, combining microscopy in living cell and yeast genetics.

2. Post-doctoral research

2.1 Experimental approach: tracking homologous loci in diploid yeast

To investigate chromatin mobility and homology search in living cells, I developed a cell biology assay in diploid budding yeast to visualize the 3-dimensional motion of a damaged DNA site as well as its homologue in living cells (Figure 9). First, we monitored the mobility of the cut locus (*tetO*/TetR-RFP) and its homologue (*lacO*/LacI-YFP) after the induction of a single I-*Sce*I DSB placed 4 kbases away from the *tetO* array (Figure 9A). Second, the DSB was induced on a different chromosomes (using HO cut site on chromosome III) while tracking the same loci (not shown here). Finally, several DSBs were induced using different does of γ-irradiations (figure 9B). In each case, the same loci, visible as a fluorescence spots, were tracked in 3 dimensions with 1 timepoint every 10 seconds; in addition, the Rad52 repair protein fused to CFP was used as a marker for the presence of DSB (Figure 9C) (Miné-Hattab, 2012).

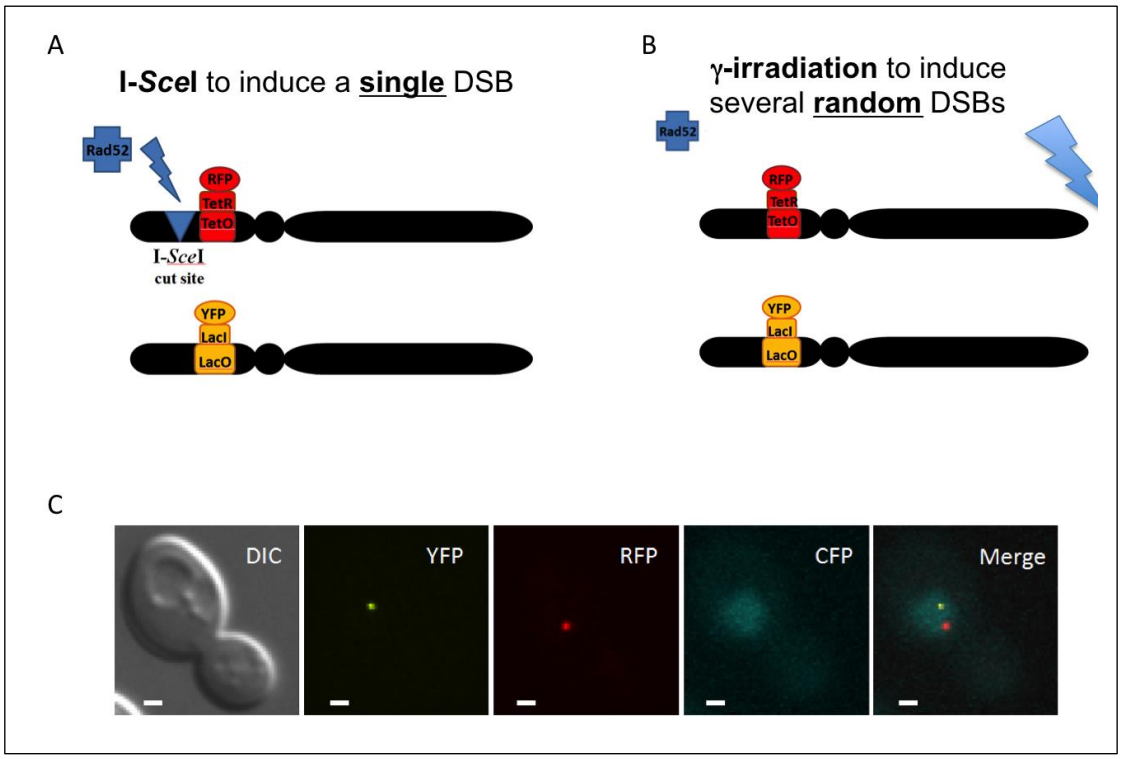

Figure 9: Description of the diploid strain used to study chromatin dynamics. (**A**) The *tetO* array (3**x**112 copies) is adjacent to an I-*Sce*I cut-site on chromosome V at *URA3*. The *lacO* array (256 copies) is at *URA3* on the other chromosome V homologue. The Rad52, TetR and LacI proteins are tagged with CFP, RFP and YFP, respectively. The strain also contains a galactose-inducible I-*Sce*I (inserted at the LYS2 locus), allowing the induction of a single DSB in the genome. (**B**) To study the genome-wide effect of DSBs, we used the same strain without the I-*Sce*I cut-site, but treated with different doses of γ-irradiations. (**C**) DIC, YFP, RFP and CFP images of the diploid strain in the absence of DSB. Flattened images of all 15 z -stacks are shown in maximum z -projection. In the absence of a DSB, there is no Rad52 focus and each chromosome V is visualized by an RFP and YFP focus. Scale bar : 1 µm.

2.2 Kinetics of homology search in living yeast

First, we used this assay to measure the kinetics of homologous pairing in living cells following the induction of a single I-*Sce*I DSB close to the *tetO* array. After 90 min of DSB induction, the first Rad52 foci colocalizing with the *tetO* array start to appear (Figure 10A) (Miné-Hattab, 2012). The homologous loci are paired in only 2.5% of the S-phase cells containing a Rad52 focus, similar to the background level of pairing in the absence of a DSB (data not shown, see (Miné-Hattab, 2012)). However, 30 minutes later (120 minutes after the beginning of the DSB induction), homologous pairing peaks with the cut locus, its homologue and the Rad52 focus colocalizing in 42 % of the S-phase cells (Figure 10B). 30 minutes later (150 minutes after the beginning of the DSB induction), paired loci decrease to 17 % of cells (see (Miné-Hattab, 2012). These results suggest that, in our system, homology search begins after ~ 90 min of induction and homologous contact can be achieved in ~ 30 minutes (this estimation is obtained from a cell population observed 90, 120 and 150 minutes after DSB induction). Next, we tracked single cells after 90 min of induction at 5-min intervals for 50 min (Figure 10C). Interestingly, after 20-25 min of tracking, the homologous loci become paired for approximately 21 ± 5 min and in most cases the Rad52 focus disassembles by the time the two loci separate (Figure 10C). We confirmed this kinetics by genomic blot and found that repair products start to appear after 120 min of DSB induction (Miné-Hattab, 2012). Combining results obtained by microscopy with the genomic blot, DNA breakage starts 30 min after induction and reaches a plateau after 90 min. At this time, Rad52 foci start to appear. The pairing between homologues peaks at 120 min and consistently, gene conversion of the cut-site starts to appear (Miné-Hattab, 2012).

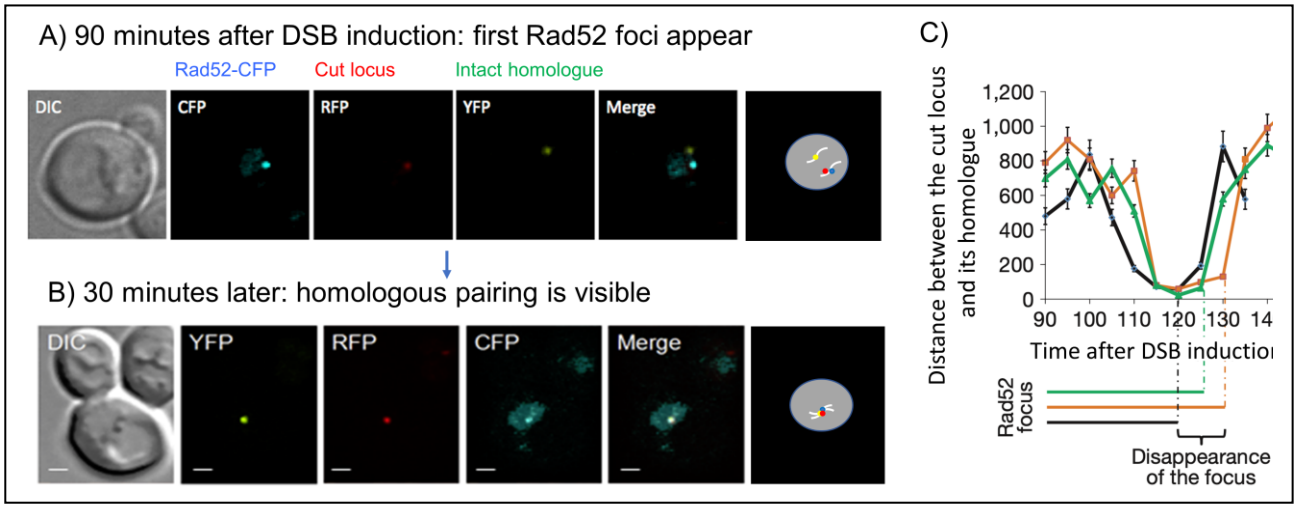

Figure 10 : Kinetics of homology search in living diploid yeast cells. A) After 90 minutes of DSB induction, early Rad52 foci appear and colocalize with the *tetO*/TetR-RFP locus harboring an I-*Sce*I cut-site (cut locus). However, the intact locus (*lacO*/LacI-YFP) is distant: we named this configuration "unpaired configuration". B) 30 minutes later: the cut locus, its homologue and the Rad52 focus colocalize in 42 % of the S-phase cells. The bar scale represents 1 μm. C) 3-D distance between the cut and its homologue through time (Δt = 5 minutes). Each color represents a different cell. The presence of a Rad52 focus is indicated below for each cell.

2.3 Increased DNA mobility facilitates homology search

How chromatin is moving between the unpaired and the paired configurations observed above? To address this question, we tracked both the cut locus and its homologue after 90 minutes of DSB induction, in cells harboring a Rad52 focus colocalizing with the *tetO* array. We found that the mobility of the damaged chromosome markedly increases, allowing it to explore a nuclear volume that is more than 10 times larger and increasing the probability of homologous pairing. Surprisingly, undamaged chromosomes (homologous or not) become also more mobile, revealing that increased chromatin exploration is a genome wide response upon DSB (Figure 11). Applying different doses of DNA damages by γ-irradiations provokes even larger chromatin mobility. Based on our results, we proposed a new view of homology search in which increased chromosome mobility facilitates homologous pairing.

Of note, our study showed that increased nuclear exploration upon DNA damage does not correlate with a higher speed of locus movement. In fact, the diffusion coefficient does not significantly change in response to damage, both at damaged and undamaged loci (Miné-Hattab and Rothstein, 2012; Mine-Hattab and Rothstein, 2013). In other words, changes in mobility allow chromatin to go further but not faster. Unfortunately, there is often a confusion in the field of chromosome dynamics: increased mobility has been often mixed with increased speed which is not what we observed.

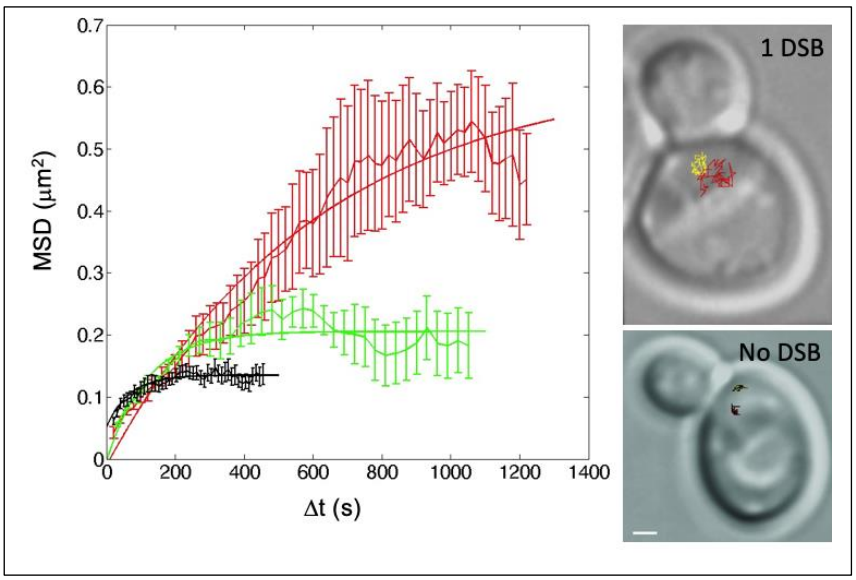

Figure 11: evidence of increased mobility both at the damaged locus and its homologue in diploid yeast. The mobility of 2 homologous loci (*URA3*) is observed during 15 minutes at 10 seconds time interval. The tracking is performed in 3-dimensions. Black : MSD curve of *URA3* loci in the absence of DNA damage. Red: MSD of cut loci (*tetO*/TetR-RFP colocalizing with a Rad52 focus) after 90 minutes of DSB induction. Green: MSD curve of its homologue (*lacO*/LacI-YFP). Right: typical nuclei are shown and trajectories of the tracked loci reveal how the exploration volume increases after DNA damage.

2.4 Multi-scales motion of chromatin and role of Rad51 during homology search

Multiple diffusion regimes simultaneously drive chromatin mobility

The following work was performed in Xavier Darzacq team during the second part of my post-doctoral training (Miné-Hattab et al., 2017). To better understand the origin of increased chromatin mobility in response to DNA damage, I used multi-scale tracking to investigate chromatin mobility at scales 10, 100 and 1000 times faster than in my previous work in the Rothstein laboratory (time-points spaced by 1000ms, 100ms and 10 ms compared to 10s in the Rothstein lab). Overall, our findings show that a single mode of diffusion is not sufficient to describe DNA motion at different time scales. Instead, upon DSB DNA motion is composed of several diffusion regimes that simultaneously drive DNA at each time scale. More specifically, in the absence of DNA damage, MSD exhibits a plateau characteristic of confined diffusion, consistent with the chromatin remaining confined inside a sub-volume of the nucleus (Heun et al., 2001; Marshall et al., 1997; Miné-Hattab, 2012). However, when observed at shorter time-intervals (10 ms to 1 s), chromatin undergoes anomalous diffusion following Rouse diffusion (anomalous exponent $\alpha = 0.5$) (Backlund et al., 2014; Hajjoul et al., 2013; Lucas et al., 2014; Miné-Hattab et al., 2017; Weber et al., 2010). In response to DSB, we have previously shown that at large time-scales (Δt =10s), chromatin confinement is dramatically increased with no significant difference in the diffusion coefficient. Here, we showed that at short time scales, damaged chromatin does not completely follow the Rouse model: instead, the cut locus exhibits an anomalous exponent of 0.58 at 1s time-interval and surprisingly, a lower mobility than undamaged chromatin at shorter time scales (100 and 10 ms). As a consequence, the MSD curve of the damaged locus crosses that of the undamaged one at time $t \sim 10$ s (Figure 12A). Such changes in the sub-diffusion mode dramatically modify the balance between surrounding and distant chromatin sampling.

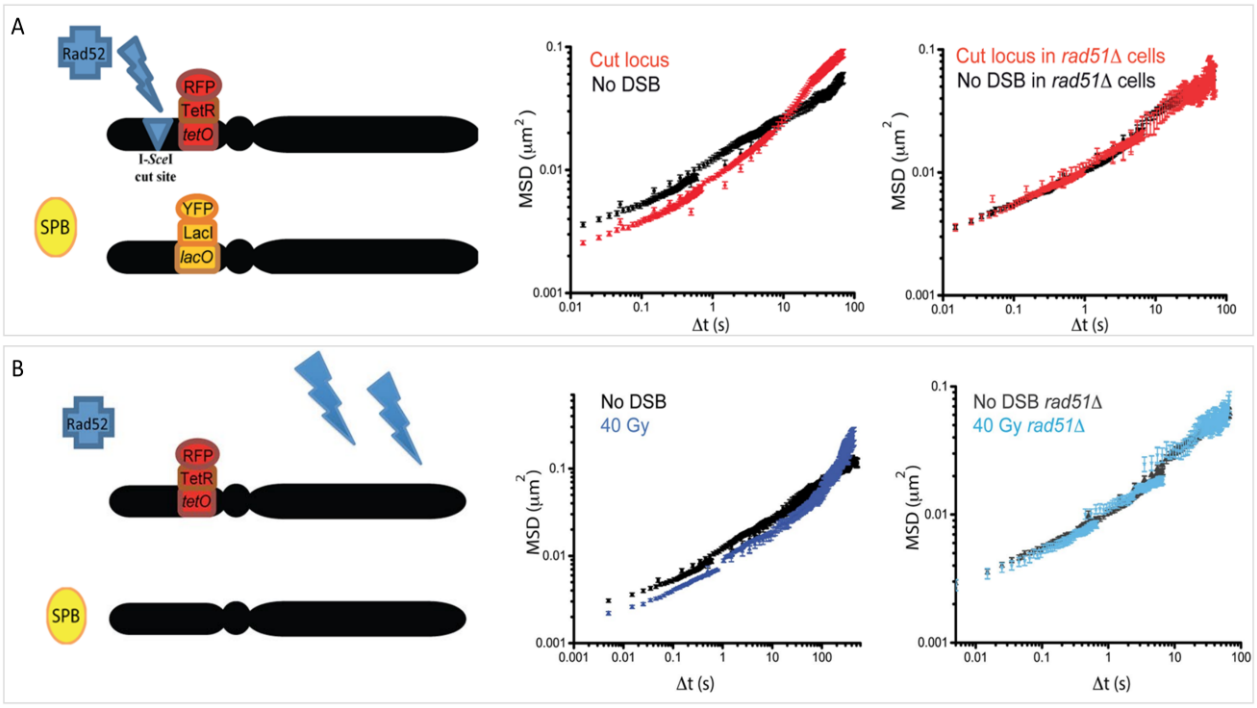

Figure 12: Scale-dependent chromatin mobility in response to DNA damage. (A) Mobility of the damaged locus. Left panel: schema of the experiment. Middle panel: MSD curves of the *URA3* locus acquired at 3 times scales: 10ms, 100ms and 1000ms time intervals. Black: cells without DNA damage. Red: cells harboring a Rad52-CFP focus colocalizing with *tetO*/TetR-RFP locus indicating the presence of a single I-*Sce*I DSB. Right

panel: similar experiment in *rad51Δ* cells. (B) Mobility of the *URA3* locus in response to random DSBs (40 Gy of γ-irradiation, equivalent to ~ 4 DSBs). Left panel: schema of the experiment. Middle panel: MSD curves of the *URA3* locus imaged at 3 times scales (10, 100 and 1000ms time intervals). Black: same curve in undamaged cells than in Figure 13A. Blue: MSD of *URA3* locus in cells harboring a Rad52-CFP focus after γ-irradiation. Right panel: similar experiment in *rad51Δ* cells.

Using $MSD \sim t^{2/D_w}$ where D_w is the dimension of the walk (Daniel ben-Avraham, 2000), we would obtain $D_{w\ noDSB} = 1.5$ compared to $D_{w\ DSB} = 1.74$ after DSB. The number of times the same site is visited is given by the relation $Dg = t^{-6/D_w}$; thus we found that a damaged locus visits less often the same sites compared. In other words, the cut locus explores the nuclear space in a less redundant manner allowing it to reach further targets faster. We conclude that, in the presence of DNA damage, the existence of multi time-scales regimes of diffusion with different parameters may reflect changes in chromatin conformation that accelerates homology search (Miné-Hattab et al., 2017). The existence of different diffusion regimes depending on the time-scale evokes the reptation model by De Gennes; however we obtained different exponents than the ones predicted by this model. So far, there is no theoretical model which can explain the exact diffusion modes we observed after DNA damage.

To investigate how the changes in diffusion affect the search time, we implemented the mean first passage time (MFPT) in complex media using the asymptotic formula expressed in (Condamin et al., 2007), extended using the explicit expression of the constants in the supplementary material. We used the formula in the case of a dimensions of the walk $d_w = \frac{2}{\alpha}$, where α is the anomalous exponent of the MSD, higher than the dimension of the space d_f. In the absence of excluded volume, we can set $d_f = 3$ and therefore the formula is valid up to the limit $\alpha < 0.66$. Explicitly, we computed the MFPT in seconds as:

$$\frac{Sd \times V \times ((D+T)^{(\frac{2}{\alpha}-d_f)} - T^{(\frac{2}{\alpha}-d_f)})}{(3/2 \times K)^{\frac{1}{\alpha}}}$$

where

- Sd is the solid angle of the section of interaction of the target (intact locus) which was arbitrary set to 1
- V is volume of the nucleus, which we set to $2.9\mu m^3$ according to http://bionumbers.hms.harvard.edu/
- D is the initial inter homologous distance, which was set 0.6µm
- T is the initial target size which was arbitrary set to 10 nm but whose value has small impact on the computed MFPT
- K is the scaling factor of the MSD, also called *anomalous diffusion coefficient.*

We computed the MFPT using the experimental values obtained by fitting the MSD for each condition: diploid without damage, diploid with a single DSB (only the cut locus is tracked) and haploid without damage. MSD were measured at different time intervals (10, 100ms and 1000ms). We obtained a MFPT of 1 to 3h only for the different parameters found for the cut locus in diploid cells while the MFPT can reach 10 to 100 hours in the absence of damage (unpublished results). The shorter MFPT (1h) corresponds to the parameters measured for the cut locus when it is observed a 1000 ms time intervals while we obtained a MFPT of ~ 3h for the cut locus observed at 100 ms and 10 ms time intervals (see Figure 13).

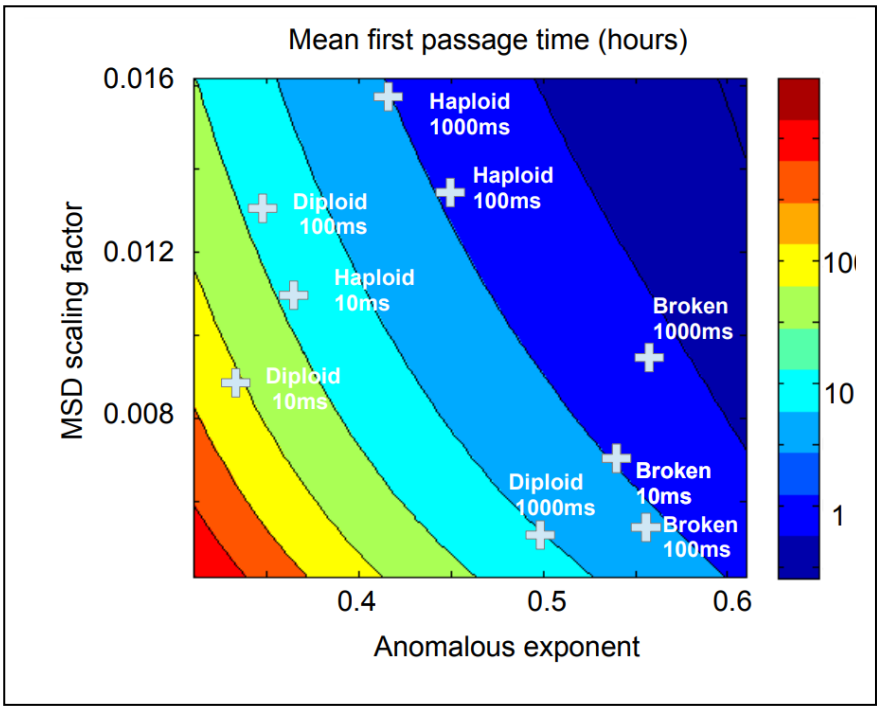

Figure 13 : Mean First Passage Time (MFPT). For all the different time scales conditions tested in Miné-Hattab et al 2017, we computed the MFPT using the anomalous exponent α and the anomalous diffusion coefficient A obtained by fitting the MSD ~ A t^{α} . "Broken" represents the results obtained for the damaged locus in diploid. "Diploid" and "haploid" represent the results obtained for the same locus (*URA3*) in the absence of DNA damage in diploid and haploid cells respectively. The timescales used to track the locus is indicated (10ms, 100ms or 1000ms).

Importantly, the existence of different regimes of diffusion depending on the time scales is not an intrinsic property of the damaged end. In response to random DSBs (40 Gy), we also observed distinct anomalous regimes, with global increased mobility at long time scales and global reduced mobility at short time scales. Such a pattern of dynamics has been described when the persistence length of a polymer increases (Faller and Müller-Plathe, 2008). Thus, our results thus suggest that chromatin is globally stiffer throughout the genome in response to DSB. This interpretation is consistent with another study using different methods in haploid yeast (Herbert et al., 2017).

Interestingly, the MSD curves of cut loci *versus* loci in undamaged cells cross at 10 s (Figure12A) whereas the ones in irradiated cells *versus* undamaged cells cross at 100 s (Figure12B). In other words, it takes 10 s on average for a broken locus to cover larger distances than in the absence of a DSB, allowing the damaged site to reach further targets; in contrast, following random DSBs, the same locus needs 100 s on average to cover larger distances than in the absence of DSBs. Thus, upon DNA damage, changes in mobility/stiffness have a stronger effect at the damaged locus than in the rest of the genome. This difference suggests that local and global changes in mobility are regulated differently. This study emphasize the importance of interrogating different spatiotemporal scales to understand chromatin motions, potentially revealing distinct dynamic processes and regulatory mechanisms.

Role of Rad51 in local and global changes in chromatin mobility/stiffness

We found that both local and global changes in mobility/stiffness are Rad51 dependent (Figure 12, rigth panels). A change in stiffness at the damaged site is consistent with the recruitment of Rad51 forming a stiff nucleofilament as observed *in vitro*. However, the role of Rad51 in genome wide mobility is not fully understood. One possibility is that the Rad51 structure moves potential dsDNA targets thus inducing a global increased mobility of the genome. Another scenario is that Rad51 triggers other modification that are spread throughout the genome and affect its mobility/stiffness (Miné-Hattab and Rothstein, 2013).

Increased mobility and its origin in the literature

Global changes of chromatin mobility on DNA damage is an intriguing phenomenon, and over the last five yeasts, several views to explain it have been proposed in the literature. They can be grouped into two classes: 1) Global increase in chromatin motion is solely due to changes of external mechanical constrains that maintain chromatin and 2) global increase in chromatin motion is due to intrinsic chromatin modifications.

To support the first view, several groups have studied the effect of centromere or telomere release on chromatin mobility. They found that centromere or telomere release alone gives a modest increase in mobility and are not sufficient to increase mobility of midarm chromosomes (Herbert et al., 2017; Lawrimore et al., 2017; Strecker et al., 2016). However, Strecker *et al*. found that a combined disruption of telomeres and centromeres can reproduce chromatin mobility observed after a DSB (Strecker et al., 2016); they identified the Mec1-dependent phosphorylation of Cep3, a kinetochore component, as an essential player in global increased chromatin mobility on DSBs. A different mechanism has been observed by Lawrimore *et al.*, who found that increased mobility of midarm chromosomes regions is microtubule dependent (Lawrimore et al., 2017). In a sense, microtubules would be responsible for a global chromatin shake-up that would be essential for global increase mobility on DSBs (Lawrimore et al., 2017). The second view is that the intrinsic properties of chromatin are modified in response to DSBs, as proposed in the "altered chromatin model" (Miné-Hattab and Rothstein, 2013) and in Seeber et al. (2014). Chromatin state can be described by distinct parameters such as rigidity, compaction, and torsion. Changes in chromatin rigidity and compaction in response DNA damage have been recently discussed in the literature, however, with different conclusions. For example, a global chromatin decompaction/relaxation has been described in mammalian cells following DNA damage (Ziv et al., 2006). More recently, the β-polymer model, as well as structured illumination microscopy imaging of a damaged locus, predicted chromatin expansion at the DSB in haploid yeast (Amitai et al., 2017; Herbert et al., 2017). Interestingly, 20-40% of the histones are degraded following DNA damage in haploid yeast. Such a loss of histones is proposed to globally increase chromatin decompaction and flexibility (Seeber et al., 2014; Hauer et al., 2017). However, this interpretation is still a matter of debate. Indeed, polymer models and STORM (stochastic optical reconstruction microscopy) imaging in haploid yeast has shown that global increased chromatin mobility on DNA damage is solely explained by an increase in chromatin rigidity without change in compaction (Herbert et al., 2017). Phosphorylation of histone H2A, which can spread over 50 kb on both sides of a DSB (Lee et al., 2014), contributes to the global increased mobility following DNA damage. Negative charges due to H2A phosphorylation might be the molecular basis of increased persistence length (García Fernández et al., 2021; Herbert et al., 2017). As Herbert *et al*. used large levels of DSBs, it remains unknown whether H2A phosphorylation in the presence of a single DSB would be enough to induced a global increase in mobility/stiffness by propagation to other chromosomes, or if it is triggered by another mechanisms. All together, no consensus has yet been reached to explain the origin of global increased mobility after DNA damage.

After my post-doctoral trainings, I joined the team of Angela Taddei at the Institute Curie (UMR3664 Nuclear Dynamics) with the project to study the changes in nuclear organization upon DNA damage using single molecule microscopy. My post-doctoral stay in Xavier Darzacq laboratory was my first contact with super resolution microscopy in 2013. There, I performed preliminary experiments using single molecule microscopy to image repair foci and histones in yeast (Rad52-mEOS2 and H2B-dendra2) as well as in human cells (histones H2B-dendra2 in primary fibroblast cells). Joining the team of Angela Taddei in 2013, we set-up a fruitful collaboration with the team of Maxime Dahan to develop single molecule microscopy in the UMR3664.

3 Permanent researcher work in Angela Taddei team

3.1Experimental approach: single resolution microscopy: PALM and SPT

Super resolution was introduced to break the fundamental diffraction limit of Light microscopy. Upon response to a point emitter source (a fluorophore/dye), microscopes produce a blurry image called the point spread function (PSF) due to the light diffraction through the optical path. As a consequence, 2 molecules closer than 100 nm are impossible to separated with ordinary inverted microscope. Super-resolution techniques break this limitation using different strategies. Here, I am using a super-resolution technique named single molecule localization microscopy, which allows the observation of single molecules at high spatial and temporal resolution (up to 20 nm/10 ms).

Photo Activable Localization Microscopy (PALM)

In 2006 2 methods of single molecule localization microscopy were conjointly developed using similar principles: PALM (Photo-Activable Localization Microscopy (Betzig et al., 2006) and STORM (Stochastic Optical Reconstruction Microscopy) (Rust et al., 2006). These approaches rely on the stochastic activation of fluorescence/dye to a bright state, which is then imaged and photobleached. Thus, very closely spaced molecules that reside in the same diffraction-limited volume (and would otherwise be spatially indistinguishable), are temporally separated. Time-merging all of the single-molecule positions obtained by repeated cycles of photoactivation followed by imaging and bleaching produce the final super-resolution reconstructed image (Figure 14A). The output image of PALM/STORM experiments gives an information on the molecules distribution at the single molecule level inside cells.

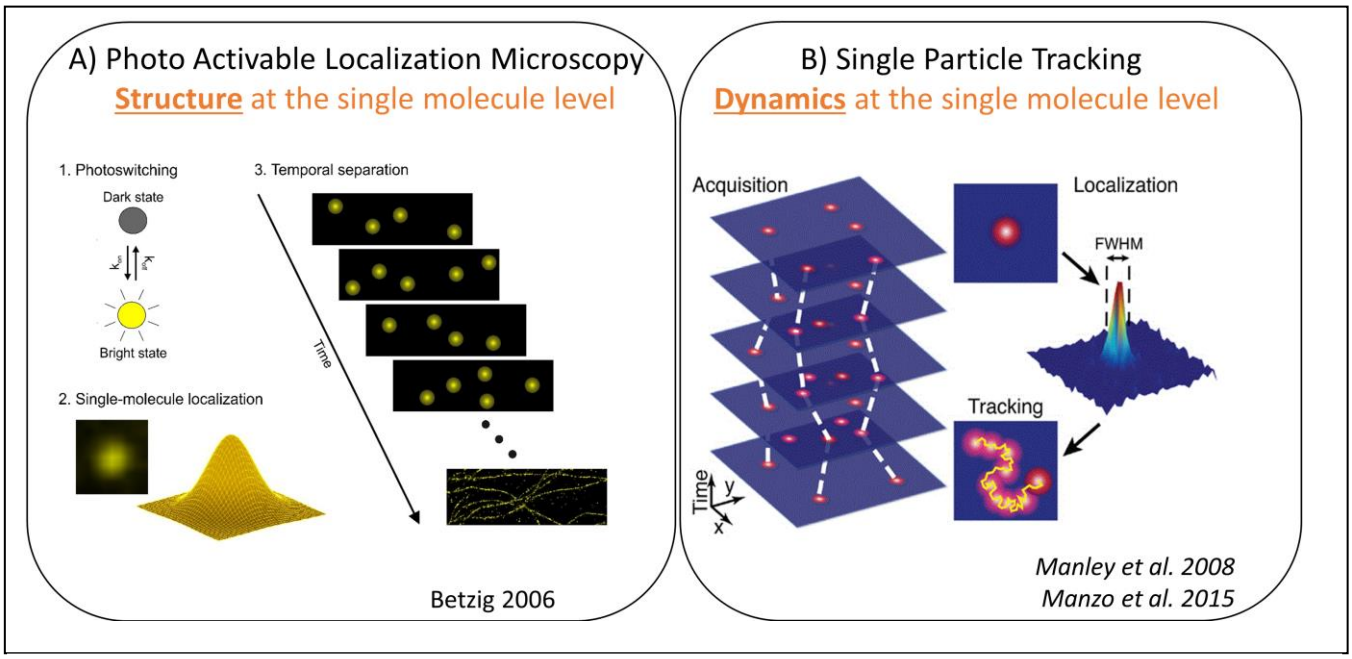

Figure 14: Principle of Photo-Activable Localization Microscopy (PALM) and Single Particle Tracking. (SPT). A) PALM: By photo-activating separately single fluorophores separated in space and fit their spatial position at high resolution, we recover a pointillist image at ~ 20 nm resolution. B) SPT: Acquisition are performed in living cells and single molecules are tracked in time at high temporal and spatial resolution (up to 10 ms and 20 nm).

Single Particle Tacking (SPT)

Watching how proteins move and interact within a living cell is crucial for better understanding their biological mechanisms. Indeed, the mode of diffusion of a moving molecule drastically changes the way it explores the available space and the time to reach a specific target destination. To complement the PALM/STORM approach, Single Particle Tracking (SPT) is a powerful technique that makes these observations possible by taking 'live' recordings of individual molecules inside living cells at high temporal and spatial resolution (up to 10 ms and 20 nm) (Manley et al., 2008; Oswald et al., 2014) (Figure 14B). Based on the way individual molecules move *in vivo*, SPT allows for i) sorting proteins into subpopulations characterized by their apparent diffusion coefficients, ii) quantifying their motion, iii) estimating residence times in specific regions of the nucleus, iv) and testing the existence of a potential attracting or repelling molecules within distances smaller than the diffraction limit.

3.2 Nuclear compartments: the physical nature of nuclear foci"

The first question I proposed to address is the internal structure and dynamics of repair foci in yeast cells. This work is fully described in 2 recent publications and a mini-review (Heltberg et al., 2021a; Miné-Hattab et al., 2020; Miné-Hattab and Taddei, 2019). The following section presents a brief summary of this work (Figure 15).

In the presence of DNA damage, repair proteins relocalize from a diffusion nuclear distribution to a condensed at the damage site: such condensates, named "foci" have been observed many years ago (Lisby et al., n.d.) but their internal structure/dynamics remain unknown. In recent years, cell compartmentalization has undergone a paradigm shift. It became clear that molecules concentrate in specific locations without the need of a membrane. However, how these membrane-less organelles are formed, maintained or disassembled remains poorly understood and several biophysical approaches started to emerge. Importantly, the physical nature of membrane-less sub-compartments is determinant for their proper function, as the deregulation of certain membrane-less compartments is tightly linked with the formation of protein aggregates related to diseases (Wang et al., 2021). A very attractive hypothesis proposed in the literature is that membrane-less compartments arise from Liquid-Liquid Phase Separation (LLPS) and form droplets (Hyman *et al*., 2014). Although some biochemical and wide field microscopy data support this hypothesis (Strom *et al.*, 2017; Altmeyer *et al.*, 2015), these observations are at the limit of the optical resolution and physical studies are still missing to discriminate this model from alternative hypothesis such as multi-valent or dynamic interactions with multiple binding sites (Miné-Hattab and Taddei, 2019). With the emergence of super resolution microscopy, it becomes possible to observe the organization and dynamics of proteins at the single molecule level inside living cells. Such data allowed us analyze the internal dynamics and organization of foci in a new light and to better understand their precise nature.

To investigate the physical nature of repair foci, we set-up a **collaboration with 3 physicists (Aleksandra Walzak, Thierry Mora and Mathias Heltberg, ENS physics**, Statistical Physics and Inference for Biology team). Together, we propose to combine our experimental single molecule approach with advanced statistical analysis: the final goal is to develop a solid framework to distinguish between several models of sub-compartments using SPT data. First, we focus on repair condensates formed by the Rad52 proteins in budding yeast. Rad52, the functional analog of human BRCA2 in yeast, stimulates the removal of RPA and recruits the Rad51 to the ssDNA tail on which it polymerizes (see introduction). By tacking individual Rad52(Halo molecules bound to JF646 dyes (Grimm et al., 2015), we compared the diffusion properties of Rad52 in different conditions: in the absence of DSB, in the presence of a single DSB inside *versus* outside foci, and in the presence of 2 individual DSBs. Overall, we found that Rad52 accumulates at DSB sites: inside repair foci, the large majority of Rad52 molecules are not bound to the ssDNA tail of the break, instead, Rad52 diffuses ~

6 times faster within repair foci than damaged chromatin, and exhibits confined motion. The Rad52 confinement radius coincides with the focus size. Moreover, foci resulting from 2 DSBs are twice larger in volume that the ones induced by a unique DSB and the Rad52 confinement radius scales accordingly. In contrast, molecules of the RPA complex (the single strand binding protein Rfa1) follow anomalous diffusion with the same diffusive properties of the focus itself or damaged chromatin. We conclude that while most Rfa1 molecules are bound to the ssDNA tail of the DSB, most of the Rad52 molecules remain free to explore the entire focus reflecting the existence of a liquid droplet around damaged DNA (Heltberg et al., 2021b; Miné-Hattab et al., 2021).

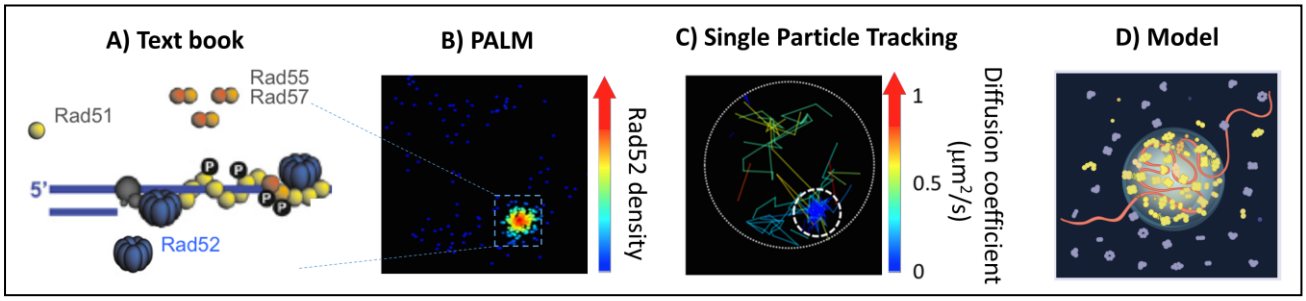

Figure 15: Single Particle Tacking used to decipher the physical nature of repair foci. A) simplified text book view of HR proteins at a damaged DNA site. B) Rad52-mMaple focus observed by live PALM. C) Diffusion map of individual Rad52-Halo molecules bound the JF646 dyes, each line represents the trajectory of an individual Rad52 molecule. D) Model inspired by our results.

We are currently using the same approach to analyze the physical nature of silencing foci, corresponding to transcriptionally-repressed regions. This work has been performed by 2 post-doctorants (***Arun Shivanandan and Susmita Sridhar***) who could not finish the project. Together with Mathias Heltberg, we are currently working on their data to compare the diffuse behavior of Sir3 molecules in different conditions. Overall, this study reveals that despite a similar aspect by conventional microscopy, silencing foci do not exhibit the hallmarks of LLPS as observed for Rad52 foci, neither the behavior observed for the repair protein RPA. We propose that silencing foci behave as polymer-polymer phase separation model (see (Miné-Hattab and Taddei, 2019)) (manuscript in preparation).

3.3 Rad51 imaging in living cells

This project started during the internship of Siyu Liu (2018) and her PhD (2019-2022)

A second project concerns the imaging of Rad51 in living yeast cells. This work started during the internship of Siyu Liu, a M2 student I supervised in 2018. Siyu Liu continued this project under the co-supervision of Angela Taddei and myself from 2019 to present (manuscript in preparation). All the data presented in this section were acquired by Siyu Liu, while I worked on the quantification of her images/movies. Many of the strains were built by **Marie Villemeur**, an engineer in the Taddei team.

The Rad51 nucleofilament has been extensively studied by *in vitro*, molecular, and genetic approaches. *In vitro*, RecA/Rad51 proteins form a right-handed helix filament around the damaged DNA (see introduction). This complex is extremely stiff since a Rad51-DNA covering only 1000 bases would form a 500 nm rod (Miné et al., 2007) which should be visible by conventional microscopy. Several studies suggested that such structure might play a crucial role for the homology search process and the strand invasion of the dsDNA (Dorfman et al., 2004; Dutreix et al., 2003; Egelman, 2001; Miné-Hattab et al., 2017). However, in the case of Rad51, very little is known about its *in vivo* structure and dynamics since no functional version of Rad51 has been yet developed despite

many trials by different expert laboratories. Several attempts to image Rad51 in budding yeast using partially functional Rad51-GFP construct indicate that Rad51 form only foci *in vivo*, but failed to observe stiff nucleofilaments resembling those observed in *in vitro* studies (Lisby et al., n.d.; Waterman et al., n.d.).

In collaboration with **Raphael Guerois** (Laboratory of Structural Biology and Radiobiology, CEA), we have recently designed a sfGFP tagged version of Rad51 in budding yeast, based on structural informations to avoid functional defects. Strains expressing this tagged version of Rad51 as unique copy show wild-type tolerance to high doses of DNA damages, opening the possibility to study functional Rad51 proteins *in vivo* for the first time. To study the structures and dynamics of Rad51 in living cells, we built strain harboring a single I-*Sce*I DSB and Rad51-sfGFP and imaged cells using conventional microscopy. First, we found that Rad51 complexes form foci and nucleofilament in living cells. The formation of Rad51 structures requires the Rad51 loader Rad52, and the extensive resection of the break by the coordinated actions of Sgs1 and Exo1 (data not shown). Second, we focused on the nucleofilaments to quantify their length, shape and dynamics in living cells in different conditions (time after DSB induction, ploidy and genetics contexts). Rad51 nucleofilament were observed both in haploid and diploid cells after the induction of a single DSB. I worked on the analysis of these data and on the quantification of the filament length and intensity (Figure 16, and Lui *et al*, manuscript in preparation). We show that the Rad51 filaments length is compatible with the coverage of Rad51 obtained by Chip around the DSB (data not shown, Lui *et al*, manuscript in preparation). Comparting haploids and diploid cells, the filaments length peaks at 4h in diploids while they continue to grow in haploid; at 6h, Rad51 filaments are much less abundant and their size start to decrease, consistent with the timing of HR previously observed (Miné-Hattab, 2012; Piazza et al., 2017).

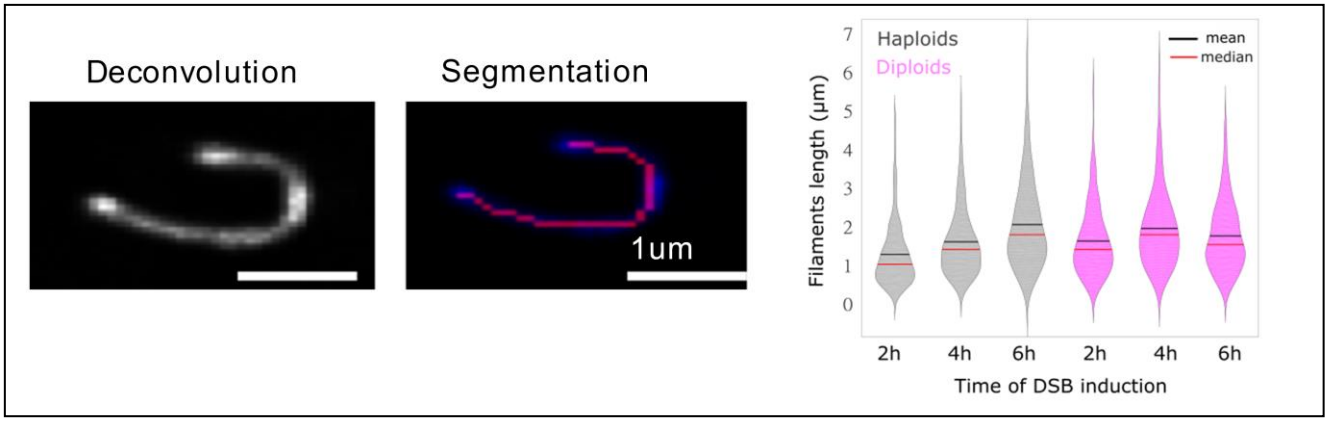

Figure 16 : Length of Rad51 nucleofilaments observed in living yeast cells. Left: typical deconvolved image of a Rad51 filament. Middle: segmentation of the Rad51 filament performed with a home-made software. Right: quantification of the filaments length observed in haploid cells (grey) and in diploid (purple) (~ 200 cells for each conditions). The filaments were observed 2h 4h and 6h after the induction of a single I-*Sce*I DSB. Data acquired by Siyu Liu.

We noticed that Rad51 filaments can adopt a variety of patterns (Figure 17) that we categorized into 5 subclasses: rods, bent filaments, circles, branched structures with a single node and others (including more complex or multiple structures). Rad51 mainly forms rod and bent filaments at the early stage after DSB induction, while other shapes, are commonly observed after a 6h of DSB induction in the wildtype strain suggesting that the simple filaments convert into more complex structures over time (data not shown). The same classes of structures were observed in diploid strain with notably a lower proportion of very complex structures (others), suggesting that the four first classes of structures are functional. Importantly, in *rad54Δ* cells, we observed nearly no branched filaments but instead, an accumulation of circular structures (>25% at 6 hours after DSB induction

versus less than 10%, in WT and *srs2Δ*, Figure 17). These Rad54 dependent branches might be related to the ability of Rad51 to promote homology search by the presynaptic complex by forming Rad54 dependent cross-bridges between dsDNA templates and the nucleofilament (Bianco et al., 2007).

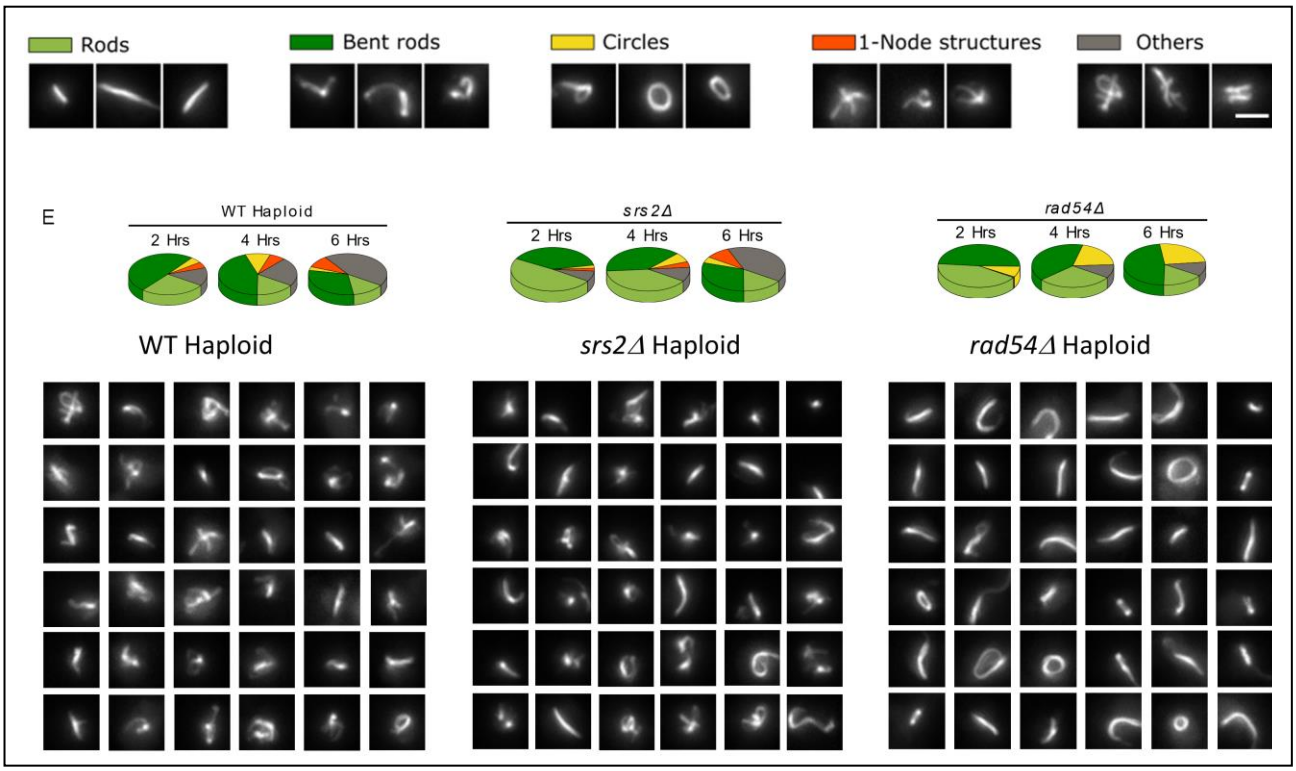

Figure 17 : Shapes of Rad51 nucleofilaments. Top: classification of the different shapes of Rad51 filaments observed in living cells. Botton: Example of Rad51 filaments observed after 6h of DSB induction in WT, *srs2D* and *rad54D* cells. (Data acquired by Siyu Liu).

To investigate the dynamics of Rad51 nucleofilaments, Siyu Liu performed time lapse movies of cells following DNA damage. By visualizing Rad51 filaments every 2 minutes 70 minutes after DSB induction, we observed abrupt changes in filament length, seemingly collapsing as bright foci, followed by a rapid re-extension (Figure 18A. In some cases, the intensity of these foci was similar to the total intensity of the filaments observed on the previous and following frames (Figure 18B). We conclude that these bright foci are folded or contracted filaments. From movies acquired at 2 or 5 minutes time intervals, the compaction of Rad51 filament occurs every 17 minutes and last 2-3 minutes in average. We proposed that the compaction of Rad51 filaments accelerate homology search (Lui *et al.*, manuscript in preparation). **Leonid Mirny** is currently developing a model for homology search based on these experimental observations.

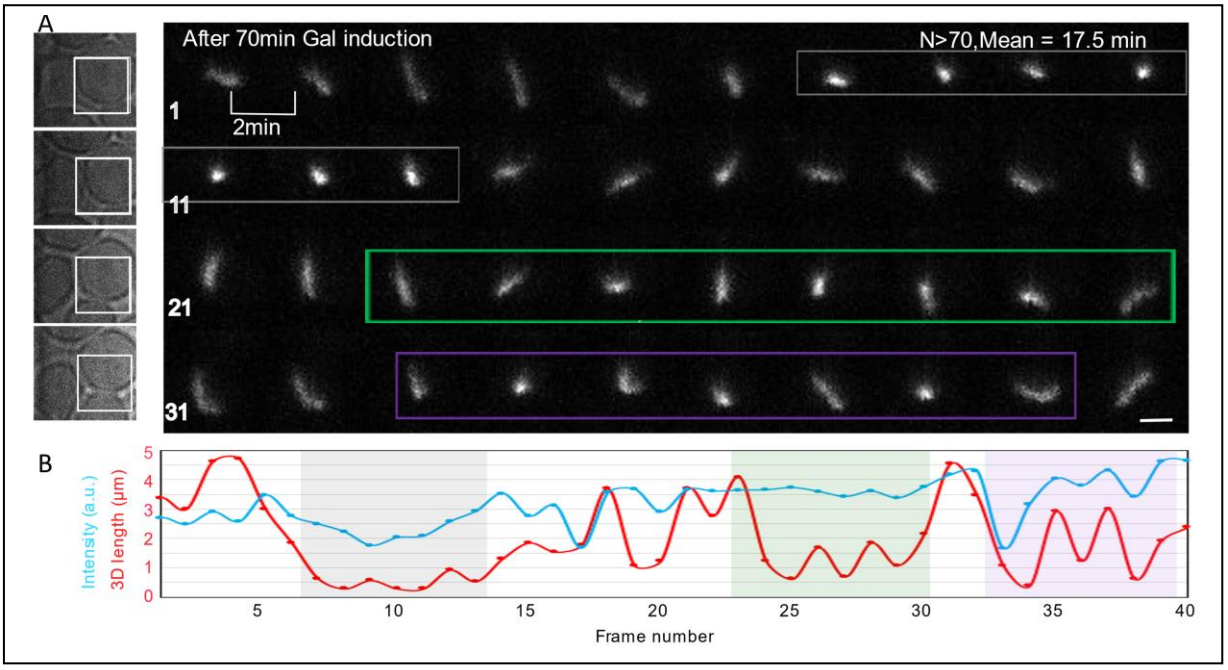

Figure 18 : Shapes of Rad51 nucleofilaments. A) Images acquired every 2 mins, 70 min after galactose addition showing Rad51 filament undergoing collapse and extension events. B) is the normalized fluorescence intensity and 3D length over time. (Data acquired by Siyu Liu).

Work performed with Fadma Lakhal: M2 student (January – June 2022)

More recently, I have worked with a M2 student (Fadma Lakhal) to investigate the fine structure and dynamics of Rad51 structures using super resolution microscopy. First, we used a spinning disk microscope combined with a live SR module (GATACA system) allowing us to reach a resolution of 180 nm in x and y in living cells. Imaging Rad51-sfGFP filaments after 4h of DSB induction in living cells at 10 s time intervals, we showed that Rad51 nucleofilaments can change shapes extremely rapidly (even between consecutive frames spaced by 10 s) (Figure 19A). Preliminary observations suggest that some filaments keep the same shape for several minutes while other filaments are extremely dynamics, changing shapes rapidly. We are currently investigating the dynamics of Rad51 filaments relative to the homologous locus in diploid cells.

We then addressed the kinetics of Rad51 filaments compaction to understand if these events could also occur at the time scale of a few seconds and would be missed in the 2 minutes time-intervals movies. Since the frequency of filaments compaction might strongly impact the kinetics of homology search, we though it was important to measure at faster time intervals the kinetics of filaments compaction. To answer this question, we imaged the dynamics of Rad51 filaments at different time intervals (10 seconds, 1 and 2 minutes) and looked specifically for cells exhibiting filament compaction events. We found that Rad51 filaments never contract and re-extend themselves in fast movies (Δt = 10s, total time = 6 minutes), indicating that filaments compaction does not occur at the timescale of a few seconds.

We then used PALM to investigate the fine structure of Rad51 nucleofilaments at 30 nm resolution. Using cells expressing Rad51-mEOS3.2 and a single I-*Sce*I DSB, we imaged filaments after 4h of DSB in fixed cells. We observed clear gaps and important width variability along the filament (Figure 19B). We are currently quantifying these images using home made software and non linear principal component analysis (NLPCA) (Figure 19C).

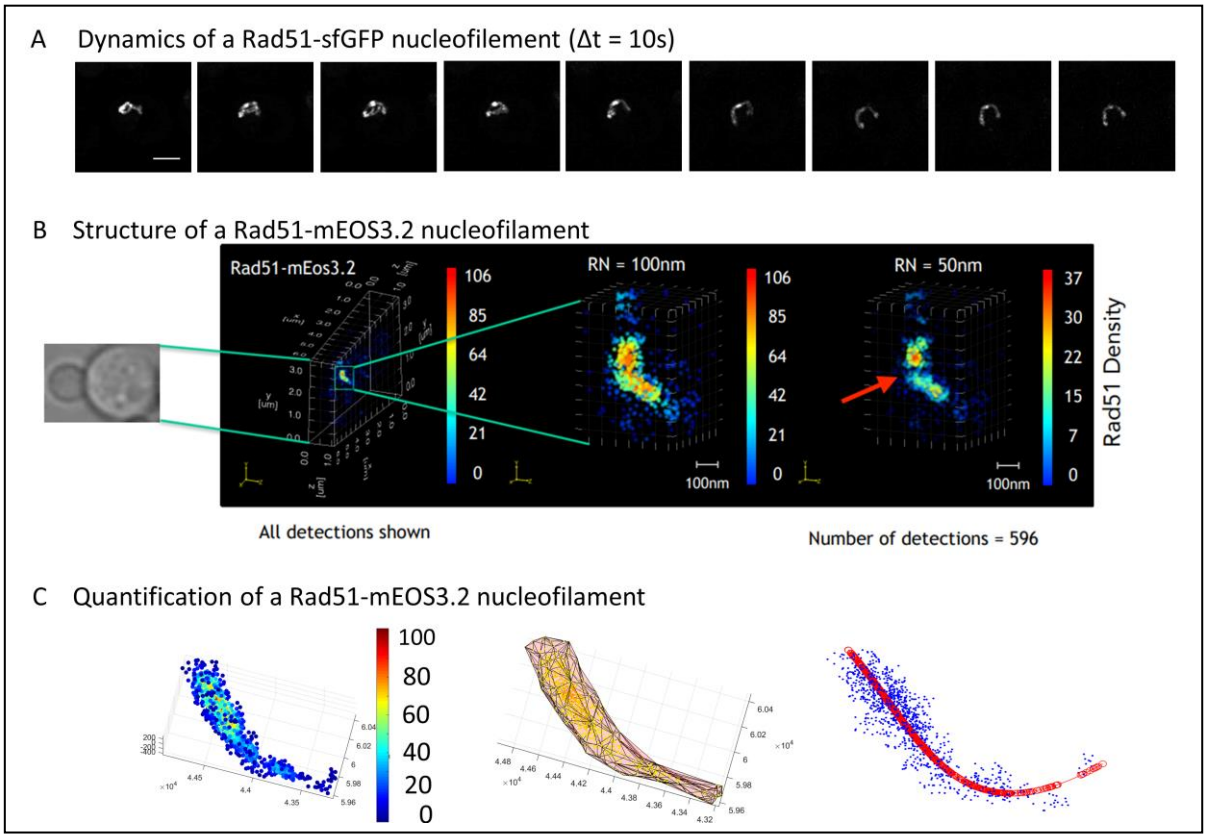

Figure 19: Rad51 filament observed at super-resolution. A) Rad51-sfGFP nucleofilament observed in haploid cells after 4h of DSB induction on spinning disk microscopy complemented by a liveSR module (GATACA system). The time interval is 10 s, the image are z-projections, the bar scale is 1 µm. B) Rad51-mEOS3.2 nucleofilament observed by PALM in a haploid cell after 4h of DSB induction. Each dot is a single Rad51 detection, the color code indicates the number of Rad51 molecules within a 100 nm or a 50 nm radius sphere (Rn: radius of neighbourhood). C) Left: Rad51-mEOS3.2 nucleofilament obtained by PALM in a haploid rad54D cell after 4h of DSB induction. Middle and Right: ongoing work to quantify the structure of this filament.

3.4 Histones organization at high resolution

Work performed in part during the internship of Manuela Baquero Perez (2018) and during her PhD (2019-2022).

A third project addresses chromatin organization using PALM approaches. Following preliminary tests performed in the Xavier Darzacq laboratory both in human and yeast cells (Figure 20A), I imaged the histone H2B by PALM in budding yeast by PALM. This approach allows us to measure the local H2B compaction and shed in light the existence of structures in different phases of the cell cycle. For that, we generated yeast strain expressing histone H2B endogenously fused with photo-activable fluorescent proteins (mMaple) (only 1 of the 2 genes coding for H2B is tagged). To represent the local changes in H2B compaction, each detection is colored as a function of its number of neighbors within a sphere of radius R_N (Figure 20B). To search for possible structures, we also use Voronoi tessellation. By partitioning the pointillist image obtained by PALM into polygons such that each polygon contains a single detection, we obtain an image in which large polygons correspond to low density regions while small polygons correspond to high density regions (Figure 20C).

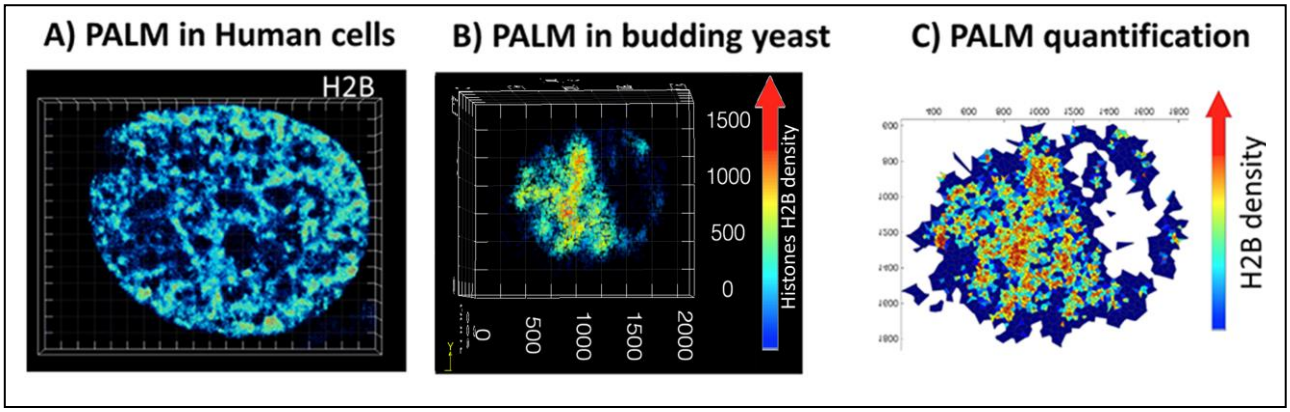

Figure 20: Investigating chromatin compaction at the single molecule level. A) Histones H2B fused to Dendra2 are visualized by PALM in U2OS cells (preliminary result performed in Xavier Dazacq team during my post-doctoral training). B) Histones H2B endogenously fused to mMaple are visualized by PALM in a S-phase haploid cell in budding yeast (Miné-Hattab, unpublished). C) Quantification of the image in B) using Voronoi diagram. The color indicates the histones density (number of neighbors within sphere of 50 nm in radius).

With a M1 student **Manuela Baquero Perez** (2018), we measured H2B compaction in wild-type cycling as well as in quiescence, a specific state of the cells observed upon starvation. Quiescent yeast cells have several characteristics, including a specific transcriptional profile, enhanced resistance to oxidative stress. The Taddei team has shown that following carbon source exhaustion, the genome of quiescent cells undergoes a major spatial re-organization. During exponential phase, silent chromatin, mainly found at the 32 telomeres, accumulates at the nuclear envelope, forming ~ 4 foci; in quiescence, telomeres relocalize to a unique "hypercluster" located in the nuclear center. Here, we propose to investigate how the rest of the genome is re-organized around this hypercluster using single molecule microscopy approaches.

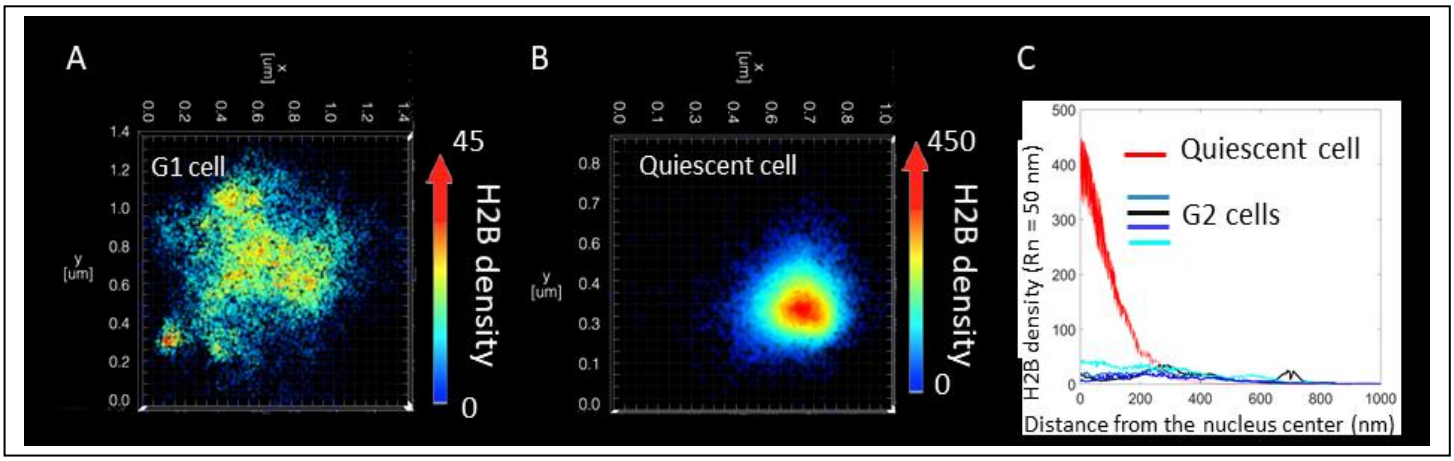

Figure 21: Density map of histones H2B measured by PALM. A) typical cell in G1. B) typical cell in quiescence. C) comparisons of 4 G1 cells (black and blue) and 1 quiescent cell (red) on the same graph. Histones densities are represented with a code color, the color indicating the number of neighbours inside a sphere of 50 nm radius (radius of neighbour Rn).

Our results revealed a completely different organization between exponential and quiescent cells: while cycling cells show fibrillar structures and high levels of lacunarity, quiescent cells show a very dense distribution of H2B that increases from the nuclear periphery to the center of the nucleus (Figure 21, unpublished). Manuela's results indicate that this massive increase in histone density is at least partially independent of telomere clustering as it is not observed in *sir3*Δ or *hho1*Δ cells. She

is continuing the project in co-supervision with Angela Taddei. In parallel to the PALM approach, she is using a chip-seq approach to investigate the transcriptional profile of quiescent cells (collaboration with Antoin Morillon team, UMR3244), and to compare the kinetics of chromatin compaction and transcription shut-down (ongoing work).

4 Future work

Thanks to an ATIP founding obtained in July 2021, I will start a new team in September 2022 at the LCQB (Laboratory of Computational and Quantitative Biology, UMR7238, IBPS). There, I would like to develop 2 axes of research:

- Investigate the changes in nuclear organization and dynamics in response to DNA damage, using single molecule microscopy both in budding yeast and in human cells. This axis is a direct continuation of my previous work.
- Address how the dynamics organization of chromatin is altered upon external mechanical stress (in particular compression) and what are the resulting consequences on genome integrity.

4.1 Changes in histones organization and dynamics in response to DNA damage

Effect of DSB on histones distribution and mobility in budding yeast

I have previously investigated how chromatin mobility is affected in response to DSB, what is the structure and dynamics of Rad52 foci, the structure Rad51-DNA complexes in living. I would like to address how chromatin organization and dynamics is affected at the level of the histones in response to DNA damage. In particular, several studies proposed that global changes chromatin mobility arise from an intrinsic change in chroamtin structure/ stiffness (Hauer and Gasser, 2017; Herbert et al., 2017; Miné-Hattab and Rothstein, 2013). Here, I propose to measure the distribution and the mobility of histones by PALM as shown in Figure 20, before and after DNA damage. Tracking H2B-mMaple histones after the induction of a single DSB, I have already observed that histones are less abundant around the damaged area (data not shown from 2016). However, the tools I used were not advanced enough to preform histones tracking. Here, I propose to track H2B-Halo histones bound to JF635, in the presence of a single DSB. Using different repair proteins as a marker for the presence of a DSB, I will be able to map how the mobility of histones is affected at different steps of HR.

Early chromatin remodeling at damaged site in human cells

Work performed by Fabiola Garcia Fernandez (post-doctorant since 2021) in collarotaion with Sébastien Huet (University of Rennes).

I then propose to address the same question in human cells. This project was born during a conference where I met Sebastien Huet (Rennes University), a biophysicist working on chromatin organization upon DNA damage in human cells. The idea of the project is to address how chromatin dynamics is altered just after DNA damage and how the first repair factors are recruited at the damaged area in human cells. To address the immediate response of the cells to DNA damage at high resolution, we imagined to combine a SPT set-up with a UV micro-laser irradiation system. This

advantage of technique is to induce DNA damage directly on cells places on the SPT microscope and to follow the mobility of individual proteins as early as 5 seconds after irradiation. Since such system is not commercially available, we have developed a custom-made set-up in collaboration with the Errol-laser company (https://www.errol-laser.com/). We are currently using this set-up in living human cells to address how histones mobility is affected a few seconds after UV-induced DNA damage, and how early repair factor are recruited at the damaged area (PARP1). Thanks to an ANR obtained with Sebastien Huet, we have recruited a post-doctorant in 2021 to work on this project (Fabiola Garcia Fernandez).

To measure the mobility of histones directly after UV-induced damages, we used U2OS cells expressing stable H2B-Halo and co-expressing iRFP670-PARP1 (Figure 22A). While histones mobility is not affected 15 seconds after UV-irradiation (IR), we found that H2B located at the irradiated zone becomes more mobile 30 seconds after IR. The effect decreases progressively until histones recover a level close to their initial mobility (Figure 22B). Importantly, this increase in nucleosome dynamics is lost in cells treated with PARPi (Olaparib), in which we observe instead reduced chromatin motion at DNA lesions. This observation suggest that histones are "trapped" by the PARPi (Figure 23).

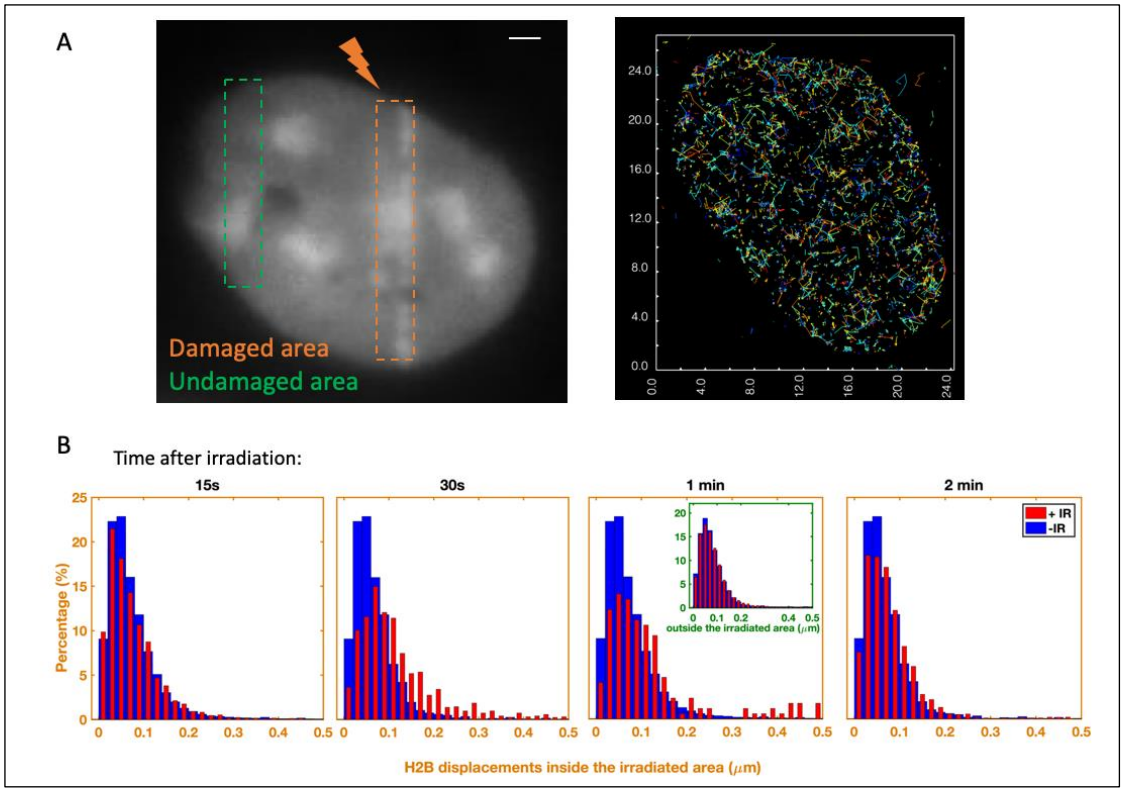

Figure 22: Changes in mobility of the histone H2B in U2OS cells observed A) PARP1 recruitment after laser irradiation in the nucleus of a U2OS cell co-expressing iRFP670-PARP1 and H2B-Halo. The yellow box represents the irradiated area and the green box corresponds to an undamaged area. Scale bar = 1 µm. B) Trajectories of individual H2B proteins fused to Halo and bound to PA-JF549, obtained by SPT. C) Histograms of histone H2B displacements measured 15s, 30s, 1 min and 2 min after UV irradiation. The time interval is 10 ms. The displacements histograms are performed from the trajectories located inside the irradiated area (orange). One minute after irradiation, we also measured the histones mobility outside of the damaged area (green box). Data acquired by Fabiola Garcia Fernandez.

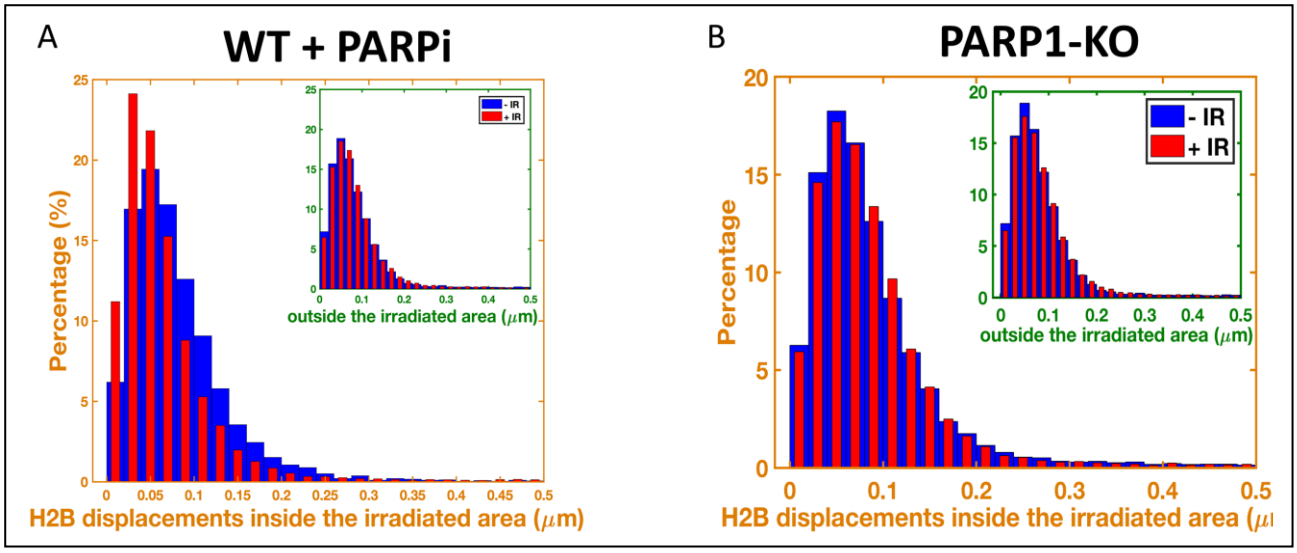

Figure 23 : H2B trapping by PARPi. A) Histogram of histones H2B displaements (H2B-Halo bound to PAFJ549) 30 s after UV irradiations, in cells treated with the PARP inhibitor Olaparib. B) Similar experiments in cells lacking PARP1 (PARP1-KO cells).

Tracking PARP1 itself after UV irradiation, we observed that PARP1 is less mobile in the damaged area but still, much more mobile than histones for example (data not shown). We are currently quantifying these results using the same methods developed for Rad52 foci and described in (Heltberg et al., 2021b; Miné-Hattab et al., 2021). In the future, we would like to quantify the diffusive behavior of other repair facts in human cells, starting with 53BP1 (involved in the NHEJ pathway) and BRAC2 (involved in the HR pathway).

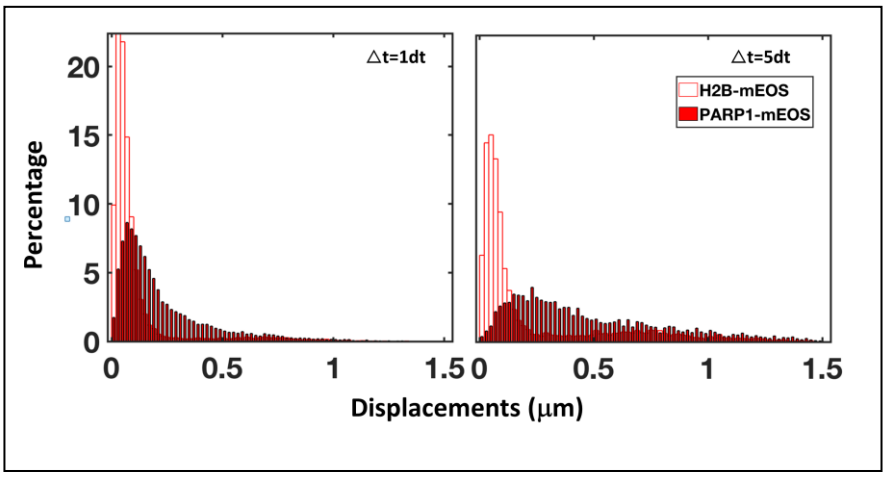

Figure 24 : Comparison of H2B and PARP1 displacements 30s after UV irradiations. Left, for 1Δt = 10ms, right, for 5Dt = 50 ms. Only tracks inside the damaged area are selected for these histograms.

4.2 Nuclear architecture in compressed cells at high resolution

Most of the studies addressing nuclear organization have been conducted in exponentially growing cell cultures: imaging is then performed on cells grown or arranged as a monolayer. In these conditions, there is still some growing space available and no particular mechanical stress. However, in the wild, cells can proliferate in a confined environment. For example, microbes often inhabit micrometer-sized pores (Holt et al., 2018), many organisms such as budding yeast grow in colonies. In mammals, several types of immune cells often migrate through dense tissues provoking nucleus deformation and DNA damage (Raab et al., 2016); tumor cells or healthy cells surrounding a tumor are exposed to different mechanical stresses (Dolega et al., 2017; Northcott et al., 2018). In these contexts, cells develop mechanical stress including shear stress, compressive and growth-induced stress.

External mechanical stress can dramatically alter essential functions of the cell: it has been shown that mechanical stress alters cell proliferation and survival (Montel et al., 2012), downregulate transcription (Damodaran et al., 2018), decrease drug penetration inside cells (Mpekris et al., 2015; Rizzuti et al., 2020), induce nuclear envelop rupture and DNA damage (Raab et al., 2016), or relocalize checkpoint proteins of DNA damage at the nuclear envelop (Kumar et al., 2014). However, how nuclear organization and dynamics are altered upon external mechanical stress and how stress affects essential functions of our genome remains poorly understood. Despite their biological importance (Alessandri et al., 2013; Delarue et al., 2014; Stylianopoulos et al., 2012), compressive mechanical stresses have been much less explored than other types of mechanical stress, for example tensile stresses, owing in part to the technical challenges of compressing cells. Thus, there is a real need to address how the dynamic organization of the nucleus is modified in confined cells and how these changes can affect fundamental biological functions.

Here, I propose to investigate how the dynamic organization of chromatin is changed upon compression, and how it affects DNA repair mechanisms. I will use an original approach combining cutting-edge microscopy at the single molecule level, micro-fluidics and genetics. I propose to use micro-fluidic chambers allowing the application of a mechanical stress on cells, on top of a super resolution microscope (Photo Activated Localization Microscopy PALM, and Single Particle Tracking SPT). Using micro-chambers developed by Morgan Delarue (ongoing collaboration, LAAS, Toulouse), it is possible to confined cells from hundreds of nanometers of bacteria to dozens of micrometers, and apply different intensities of mechanical stresses, from the kPa range of mammalian cells to the 100 kPa of yeasts.

To have a comprehensive view of how stress affect molecular organization and diffusion, I propose to use a multi-scale approach from the single molecule level, the level of individual gene to a whole chromosome scale both in yeast *Saccharomyces cerevisiae* and human cells. Yeast provides a powerful model system for genetics and allows the design of powerful experiments to better understand the mechanisms of HR. Furthermore, yeast can develop compressive stress inside a colony, when grown in a rigid porous environment(Holt et al., 2018) or simply during mitosis. **Using the range of compressive stress found in nature**, our preliminary results show that compression already affects the size of yeast nucleus. Most of the experiments will also be performed in human cells, which often handle compression *in situ*, the pipelines and the genetics performed in yeast allowing faster progress.

We will develop 3 approaches allowing the imaging of:

i) the dynamic organization of histones and repair proteins at the single molecule level
ii) the diffusion of specific chromosomal loci,
iii) the conformation and rigidity of a whole chromosome.

Altogether, our results will allow us to draw a precise picture of the nuclear organization in cells under compression, and to better understand the consequences of compression on genome integrity and on the mechanism of DSB repair. To summarize, the questions I will address are the following:

- Aim 1: How does pressure affect nuclear organization ?

First, we will address how nuclear organization is affected in cells under compression, in yeast *Saccharomyces cerevisiae* and human cells. Using our multi-scale imaging approach, we will directly access: how compression modifies histones compaction and dynamics, genes positioning and mobility inside the nucleus, and chromosome conformation and rigidity.

- Aim 2: How does pressure affect DNA repair ?

Second, we will investigate if compression can induce DSBs *per se* and lead to the formation of repair foci in yeast and human cells. We well test several intensities of pressure to see if DSBs can occur for a certain threshold of compression. Since the dynamic organization of chromatin is essential for HR, we will test how the kinetics of HR is altered upon compression, in particular: does compression affect the formation of repair foci and their LLPS properties, how the kinetics of homology search is affected, does compression increases the clustering of multiple DSBs and chromosomal translocations?

- Aim 3: at a longer term, what is the link between the cytoskeletal response to compression and changes in chromatin dynamics and structures ?

Cell compression will not only exert a direct mechanical effect on the nucleus and its contents, but also likely trigger stress and mechanosensitive responses involving membrane channels, changes in cytosolic crowding, and cytoskeletal responses. In recent years, there has been a surge of research investigating those effects with various advanced confinement assays. All of those effects in turn can affect chromatin dynamics and structure.

Conclusions

Throughout my career, I have worked on the mechanisms of DNA repair using inter-disciplinary and multi-scales approaches. From my research work, designing new experiments and trying new approaches make each day stimulating and challenging. I am enthusiastic to be able to transmit this spirit to the next generation of researchers.

REFERENCES

Alessandri, K., Sarangi, B.R., Gurchenkov, V.V., Sinha, B., Kiessling, T.R., Fetler, L., Rico, F., Scheuring, S., Lamaze, C., Simon, A., Geraldo, S., Vignjevic, D., Domejean, H., Rolland, L., Funfak, A., Bibette, J., Bremond, N., Nassoy, P., 2013. Cellular capsules as a tool for multicellular spheroid production and for investigating the mechanics of tumor progression in vitro. Proc. Natl. Acad. Sci. 110, 14843–14848. https://doi.org/10.1073/pnas.1309482110

Andrews, S.S., 2014. Methods for modeling cytoskeletal and DNA filaments. Phys Biol 18.

Arata, H., Takahashi, M., Viovy, J.-L., Cappello, G., n.d. Direct observation of twisting steps during Rad51 polymerization on DNA. PNAS 6.

Arenson, T.A., Tsodikov, O.V., Cox, M.M., 1999. Quantitative analysis of the kinetics of end-dependent disassembly of RecA filaments from ssDNA. J. Mol. Biol. 288, 391–401. https://doi.org/10.1006/jmbi.1999.2705

Backlund, M.P., Joyner, R., Weis, K., Moerner, W.E., 2014. Correlations of three-dimensional motion of chromosomal loci in yeast revealed by the double-helix point spread function microscope. Mol. Biol. Cell 25, 11.

Barzel, A., Kupiec, M., 2008. Finding a match: how do homologous sequences get together for recombination? Nat. Rev. Genet. 9, 27–37. https://doi.org/10.1038/nrg2224

Benson, F.E., Stasiak, A., West, S.C., 1994. Purification and characterization of the human Rad51 protein, an analogue of E. coli RecA. EMBO J. 13, 5764–5771. https://doi.org/10.1002/j.1460-2075.1994.tb06914.x

Betzig, E., Patterson, G.H., Sougrat, R., Lindwasser, O.W., Olenych, S., Bonifacino, J.S., Davidson, M.W., Lippincott-Schwartz, J., Hess, H.F., 2006. Imaging Intracellular Fluorescent Proteins at Nanometer Resolution. Science 313, 1642–1645. https://doi.org/10.1126/science.1127344

Bianco, P.R., Bradfield, J.J., Castanza, L.R., Donnelly, A.N., 2007. Rad54 Oligomers Translocate and Cross-bridge Double-stranded DNA to Stimulate Synapsis. J. Mol. Biol. 374, 618–640. https://doi.org/10.1016/j.jmb.2007.09.052

Bouchiat, C., Wang, M.D., Allemand, J.-F., Strick, T., Block, S.M., Croquette, V., 1999. Estimating the Persistence Length of a Worm-Like Chain Molecule from Force-Extension Measurements. Biophys. J. 76, 409–413. https://doi.org/10.1016/S0006-3495(99)77207-3

Chi, P., Van Komen, S., Sehorn, M.G., Sigurdsson, S., Sung, P., 2006. Roles of ATP binding and ATP hydrolysis in human Rad51 recombinase function. DNA Repair 5, 381–391. https://doi.org/10.1016/j.dnarep.2005.11.005

Condamin, S., Bénichou, O., Tejedor, V., Voituriez, R., Klafter, J., 2007. First-passage times in complex scale-invariant media. Nature 450, 77–80. https://doi.org/10.1038/nature06201

Conway, A.B., Lynch, T.W., Zhang, Y., Fortin, G.S., Fung, C.W., Symington, L.S., Rice, P.A., 2004. Crystal structure of a Rad51 filament. Nat. Struct. Mol. Biol. 11, 791–796. https://doi.org/10.1038/nsmb795

Damodaran, K., Venkatachalapathy, S., Alisafaei, F., Radhakrishnan, A.V., Jokhun, D.S., Shenoy, V.B., Shivashankar, G.V., 2018. Compressive force induces reversible chromatin condensation and cell geometry–dependent transcriptional response. Mol. Biol. Cell 29, 13.

Daniel ben-Avraham, 2000. Diffusion and Reactions in Fractals and Disordered Systems.

Delarue, M., Montel, F., Vignjevic, D., Prost, J., Joanny, J.-F., Cappello, G., 2014. Compressive Stress Inhibits Proliferation in Tumor Spheroids through a Volume Limitation. Biophys. J. 107, 1821–1828. https://doi.org/10.1016/j.bpj.2014.08.031

Disseau, L., Miné, J., Dilhan, M., Camon, H., Viovy, J.-L., 2009. A Novel Way To Combine Magnetic Tweezers and Fluorescence Microscopy For Single Molecule Studies. Biophys. J. 96, 556a. https://doi.org/10.1016/j.bpj.2008.12.3652

Dolega, M.E., Delarue, M., Ingremeau, F., Prost, J., Delon, A., Cappello, G., 2017. Cell-like pressure sensors reveal increase of mechanical stress towards the core of multicellular spheroids under compression. Nat. Commun. 8, 14056. https://doi.org/10.1038/ncomms14056

Dorfman, K.D., Fulconis, R., Dutreix, M., Viovy, J.-L., 2004. Model of RecA-Mediated Homologous Recognition. Phys. Rev. Lett. 93, 268102. https://doi.org/10.1103/PhysRevLett.93.268102

Dubarry, M., Loïodice, I., Chen, C.L., Thermes, C., Taddei, A., 2011. Tight protein–DNA interactions favor gene silencing. Genes Dev. 25, 1365–1370. https://doi.org/10.1101/gad.611011

Dupaigne, P., Lavelle, C., Justome, A., Lafosse, S., Mirambeau, G., Lipinski, M., Piétrement, O., Le Cam, E., 2008. Rad51 Polymerization Reveals a New Chromatin Remodeling Mechanism. PLoS ONE 3, e3643. https://doi.org/10.1371/journal.pone.0003643

Dutreix, M., Fulconis, R., Viovy, J.-L., 2003. The Search for Homology: A Paradigm for Molecular Interactions? Complexus 1, 89–99. https://doi.org/10.1159/000070465

Egelman, E.H., 2001. Does a Stretched DNA Structure Dictate the Helical Geometry of RecA-like Filaments? J. Mol. Biol. 309, 539–542. https://doi.org/10.1006/jmbi.2001.4686

Fulconis, R., Mine, J., Bancaud, A., Dutreix, M., Viovy, J.-L., 2006. Mechanism of RecA-mediated homologous recombination revisited by single molecule nanomanipulation. EMBO J. 25, 4293–4304. https://doi.org/10.1038/sj.emboj.7601260

García Fernández, F., Lemos, B., Khalil, Y., Batrin, R., Haber, J.E., Fabre, E., 2021. Modified chromosome structure caused by phosphomimetic H2A modulates the DNA damage response by increasing chromatin mobility in yeast. J. Cell Sci. 134, jcs258500. https://doi.org/10.1242/jcs.258500

Grimm, J.B., English, B.P., Chen, J., Slaughter, J.P., Zhang, Z., Revyakin, A., Patel, R., Macklin, J.J., Normanno, D., Singer, R.H., Lionnet, T., Lavis, L.D., 2015. A general method to improve fluorophores for live-cell and single-molecule microscopy. Nat. Methods 12, 244–250. https://doi.org/10.1038/nmeth.3256

Hajjoul, H., Mathon, J., Ranchon, H., Goiffon, I., Mozziconacci, J., Albert, B., Carrivain, P., Victor, J.-M., Gadal, O., Bystricky, K., Bancaud, A., 2013. High-throughput chromatin motion tracking in living yeast reveals the flexibility of the fiber throughout the genome. Genome Res. 23, 1829–1838. https://doi.org/10.1101/gr.157008.113

Hauer, M.H., Gasser, S.M., 2017. Chromatin and nucleosome dynamics in DNA damage and repair. Genes Dev. 31, 2204–2221. https://doi.org/10.1101/gad.307702.117

Hegner, M., Smith, S.B., Bustamante, C., 1999. Polymerization and mechanical properties of single RecA–DNA filaments. Proc. Natl. Acad. Sci. 96, 10109–10114. https://doi.org/10.1073/pnas.96.18.10109

Heltberg, M.L., Mine-Hattab, J., Taddei, A., Walczak, A.M., Mora, T., 2021a. Physical observables to determine the nature of membrane-less cellular sub-compartments (preprint). Biophysics. https://doi.org/10.1101/2021.04.01.438041

Heltberg, M.L., Miné-Hattab, J., Taddei, A., Walczak, A.M., Mora, T., 2021b. Physical observables to determine the nature of membrane-less cellular sub-compartments. eLife 10, e69181. https://doi.org/10.7554/eLife.69181

Herbert, S., Brion, A., Arbona, J., Lelek, M., Veillet, A., Lelandais, B., Parmar, J., Fernández, F.G., Almayrac, E., Khalil, Y., Birgy, E., Fabre, E., Zimmer, C., 2017. Chromatin stiffening underlies enhanced locus mobility after DNA damage in budding yeast. EMBO J. 36, 2595–2608. https://doi.org/10.15252/embj.201695842

Heun, P., Laroche, T., Shimada, K., Furrer, P., Gasser, S.M., 2001. Chromosome Dynamics in the Yeast Interphase Nucleus. Science 294, 2181–2186. https://doi.org/10.1126/science.1065366

Holt, L.J., Hallatschek, O., Delarue, M., 2018. Mechano-chemostats to study the effects of compressive stress on yeast, in: Methods in Cell Biology. Elsevier, pp. 215–231. https://doi.org/10.1016/bs.mcb.2018.06.010

Jacome, A., Fernandez-Capetillo, O., 2011. Lac operator repeats generate a traceable fragile site in mammalian cells. EMBO Rep. 12, 1032–1038. https://doi.org/10.1038/embor.2011.158

Klein, H.L., Bačinskaja, G., Che, J., Cheblal, A., Elango, R., Epshtein, A., Fitzgerald, D.M.,

Gómez-González, B., Khan, S.R., Kumar, S., Leland, B.A., Mei, Q., Miné-Hattab, J., Piotrowska, A., Polleys, E.J., Radchenko, E.A., Saada, A.A., Sakofsky, C.J., Shim, E.Y., Xia, J., Yan, Z., Yin, Y., Aguilera, A., Argueso, J.L., Gasser, S.M., Gordenin, D.A., Haber, J.E., Ira, G., King, M.C., Kolodner, R.D., Kuzminov, A., Lambert, S.A., Lee, S.E., Miller, K.M., Mirkin, S.M., Petes, T.D., Rosenberg, S.M., Symington, L.S., Zawadzki, P., Kim, N., Lisby, M., 2019. Guidelines for DNA recombination and repair studies: Cellular assays of DNA repair pathways. OPEN ACCESS 6, 64.

Kumar, A., Mazzanti, M., Mistrik, M., Kosar, M., Beznoussenko, G.V., Mironov, A.A., Garrè, M., Parazzoli, D., Shivashankar, G.V., Scita, G., Bartek, J., Foiani, M., 2014. ATR Mediates a Checkpoint at the Nuclear Envelope in Response to Mechanical Stress. Cell 158, 633–646. https://doi.org/10.1016/j.cell.2014.05.046

Lawrimore, J., Barry, T.M., Barry, R.M., York, A.C., Friedman, B., Cook, D.M., Akialis, K., Tyler, J., Vasquez, P., Yeh, E., Bloom, K., 2017. Microtubule dynamics drive enhanced chromatin motion and mobilize telomeres in response to DNA damage. Mol. Biol. Cell 28, 1701–1711. https://doi.org/10.1091/mbc.e16-12-0846

Leger, J.F., Robert, J., Bourdieu, L., Chatenay, D., Marko, J.F., 1998. RecA binding to a single double-stranded DNA molecule: A possible role of DNA conformational fluctuations. Proc. Natl. Acad. Sci. 95, 12295–12299. https://doi.org/10.1073/pnas.95.21.12295

Lisby, M., Barlow, J.H., Burgess, R.C., Rothstein, R., n.d. Choreography of the DNA Damage Response: Spatiotemporal Relationships among Checkpoint and Repair Proteins 15.

Lucas, J.S., Zhang, Y., Dudko, O.K., Murre, C., 2014. 3D Trajectories Adopted by Coding and Regulatory DNA Elements: First-Passage Times for Genomic Interactions. Cell 158, 339–352. https://doi.org/10.1016/j.cell.2014.05.036

Manley, S., Gillette, J.M., Patterson, G.H., Shroff, H., Hess, H.F., Betzig, E., Lippincott-Schwartz, J., 2008. High-density mapping of single-molecule trajectories with photoactivated localization microscopy. Nat. Methods 5, 155–157. https://doi.org/10.1038/nmeth.1176

Marshall, W.F., Straight, A., Marko, J.F., Swedlow, J., Dernburg, A., Belmont, A., Murray, A.W., Agard, D.A., Sedat, J.W., 1997. Interphase chromosomes undergo constrained diffusional motion in living cells. Curr. Biol. 7, 930–939. https://doi.org/10.1016/S0960-9822(06)00412-X

Michalet, X., 2011. Mean Square Displacement Analysis of Single-Particle Trajectories with Localization Error: Brownian Motion in Isotropic Medium 26.

Miné, J., Disseau, L., Takahashi, M., Cappello, G., Dutreix, M., Viovy, J.-L., 2007. Real-time measurements of the nucleation, growth and dissociation of single Rad51–DNA nucleoprotein filaments. Nucleic Acids Res. 35, 7171–7187. https://doi.org/10.1093/nar/gkm752

Miné-Hattab, J., 2012. Increased chromosome mobility facilitates homology search during recombination 10.

Miné-Hattab, J., Fleury, G., Prevost, C., Dutreix, M., Viovy, J.-L., 2011. Optimizing the Design of Oligonucleotides for Homology Directed Gene Targeting. PLoS ONE 6, e14795. https://doi.org/10.1371/journal.pone.0014795

Miné-Hattab, J., Heltberg, M., Villemeur, M., Guedj, C., Mora, T., Walczak, A.M., Dahan, M., Taddei, A., 2021. Single molecule microscopy reveals key physical features of repair foci in living cells. eLife 10, e60577. https://doi.org/10.7554/eLife.60577

Miné-Hattab, J., Heltberg, M., Villemeur, M., Guedj, C., Mora, T., Walczak, A.M., Dahan, M., Taddei, A., 2020. Single molecule microscopy reveals key physical features of repair foci in living cells (preprint). Biophysics. https://doi.org/10.1101/2020.06.18.160085

Miné-Hattab, J., Recamier, V., Izeddin, I., Rothstein, R., Darzacq, X., 2017. Multi-scale tracking reveals scale-dependent chromatin dynamics after DNA damage. Mol. Biol. Cell 28, 3323–3332. https://doi.org/10.1091/mbc.e17-05-0317

Miné-Hattab, J., Rothstein, R., 2013. DNA in motion during double-strand break repair. Trends Cell Biol. 23, 529–536. https://doi.org/10.1016/j.tcb.2013.05.006

Miné-Hattab, J., Taddei, A., 2019. Physical principles and functional consequences of nuclear compartmentalization in budding yeast. Curr. Opin. Cell Biol. 58, 105–113. https://doi.org/10.1016/j.ceb.2019.02.005

Modesti, M., Ristic, D., van der Heijden, T., Dekker, C., van Mameren, J., Peterman, E.J.G., Wuite, G.J.L., Kanaar, R., Wyman, C., 2007. Fluorescent Human RAD51 Reveals Multiple Nucleation Sites and Filament Segments Tightly Associated along a Single DNA Molecule. Structure 15, 599–609. https://doi.org/10.1016/j.str.2007.04.003

Montel, F., Delarue, M., Elgeti, J., Vignjevic, D., Cappello, G., Prost, J., 2012. Isotropic stress reduces cell proliferation in tumor spheroids. New J. Phys. 14, 055008. https://doi.org/10.1088/1367-2630/14/5/055008

Mpekris, F., Angeli, S., Pirentis, A.P., Stylianopoulos, T., 2015. Stress-mediated progression of solid tumors: effect of mechanical stress on tissue oxygenation, cancer cell proliferation, and drug delivery. Biomech. Model. Mechanobiol. 14, 1391–1402. https://doi.org/10.1007/s10237-015-0682-0

Northcott, J.M., Dean, I.S., Mouw, J.K., Weaver, V.M., 2018. Feeling Stress: The Mechanics of Cancer Progression and Aggression. Front. Cell Dev. Biol. 6, 17. https://doi.org/10.3389/fcell.2018.00017

Oswald, F., L. M. Bank, E., Bollen, Y.J.M., Peterman, E.J.G., 2014. Imaging and quantification of trans-membrane protein diffusion in living bacteria. Phys Chem Chem Phys 16, 12625–12634. https://doi.org/10.1039/C4CP00299G

Pastink, A., Eeken, J.C.J., Lohman, P.H.M., 2001. Genomic integrity and the repair of double-strand DNA breaks. Mutat. Res. Mol. Mech. Mutagen. 480–481, 37–50. https://doi.org/10.1016/S0027-5107(01)00167-1

Piazza, A., Wright, W.D., Heyer, W.-D., 2017. Multi-invasions Are Recombination Byproducts that Induce Chromosomal Rearrangements. Cell 170, 760-773.e15. https://doi.org/10.1016/j.cell.2017.06.052

Pierobon, P., Miné-Hattab, J., Cappello, G., Viovy, J.-L., Lagomarsino, M.C., 2010. Separation of time scales in one-dimensional directed nucleation-growth processes. Phys. Rev. E 82, 061904. https://doi.org/10.1103/PhysRevE.82.061904

Raab, M., Gentili, M., de Belly, H., Thiam, H.-R., Vargas, P., Jimenez, A.J., Lautenschlaeger, F., Voituriez, R., Lennon-Dumenil, A.-M., Manel, N., Piel, M., 2016. ESCRT III repairs nuclear envelope ruptures during cell migration to limit DNA damage and cell death. Science 352, 359–362. https://doi.org/10.1126/science.aad7611

Rizzuti, I.F., Mascheroni, P., Arcucci, S., Ben-Mériem, Z., Prunet, A., Barentin, C., Rivière, C., Delanoë-Ayari, H., Hatzikirou, H., Guillermet-Guibert, J., Delarue, M., 2020. Mechanical Control of Cell Proliferation Increases Resistance to Chemotherapeutic Agents. Phys. Rev. Lett. 125, 128103. https://doi.org/10.1103/PhysRevLett.125.128103

Rust, M.J., Bates, M., Zhuang, X., 2006. Sub-diffraction-limit imaging by stochastic optical reconstruction microscopy (STORM). Nat. Methods 3, 793–796. https://doi.org/10.1038/nmeth929

Saad, H., Gallardo, F., Dalvai, M., Tanguy-le-Gac, N., Lane, D., Bystricky, K., 2014. DNA Dynamics during Early Double-Strand Break Processing Revealed by Non-Intrusive Imaging of Living Cells. PLoS Genet. 10, e1004187. https://doi.org/10.1371/journal.pgen.1004187

Sagi, D., Tlusty, T., Stavans, J., 2006. High fidelity of RecA-catalyzed recombination: a watchdog of genetic diversity. Nucleic Acids Res. 34, 5021–5031. https://doi.org/10.1093/nar/gkl586

Shivashankar, G.V., Feingold, M., Krichevsky, O., Libchaber, A., 1999. RecA polymerization on double-stranded DNA by using single-molecule manipulation: The role of ATP hydrolysis. Proc. Natl. Acad. Sci. 96, 7916–7921. https://doi.org/10.1073/pnas.96.14.7916

Strecker, J., Gupta, G.D., Zhang, W., Bashkurov, M., Landry, M.-C., Pelletier, L., Durocher, D., 2016. DNA damage signalling targets the kinetochore to promote chromatin mobility. Nat. Cell Biol. 18, 281–290. https://doi.org/10.1038/ncb3308

Stylianopoulos, T., Martin, J.D., Chauhan, V.P., Jain, S.R., Diop-Frimpong, B., Bardeesy, N., Smith, B.L., Ferrone, C.R., Hornicek, F.J., Boucher, Y., Munn, L.L., Jain, R.K., 2012. Causes, consequences, and remedies for growth-induced solid stress in murine and human tumors. Proc. Natl. Acad. Sci. 109, 15101–15108. https://doi.org/10.1073/pnas.1213353109

Tombline, G., Fishel, R., 2002. Biochemical Characterization of the Human RAD51 Protein. J. Biol. Chem. 277, 14417–14425. https://doi.org/10.1074/jbc.M109915200

Turner, M.S., 2000. Two Time Constants for the Binding of Proteins to DNA from Micromechanical Data. Biophys. J. 78, 600–607. https://doi.org/10.1016/S0006-3495(00)76620-3

Vilenchik, M.M., Knudson, A.G., 2003. Endogenous DNA double-strand breaks: Production, fidelity of repair, and induction of cancer. Proc. Natl. Acad. Sci. 100, 12871–12876. https://doi.org/10.1073/pnas.2135498100

Wang, B., Zhang, Lei, Dai, T., Qin, Z., Lu, H., Zhang, Long, Zhou, F., 2021. Liquid–liquid phase separation in human health and diseases. Signal Transduct. Target. Ther. 6, 290. https://doi.org/10.1038/s41392-021-00678-1

Waterman, D.P., Zhou, F., Li, K., Lee, C.-S., Tsabar, M., Eapen, V.V., Mazzella, A., Haber, J.E., n.d. Live cell monitoring of double strand breaks in S. cerevisiae 22.

Weber, S.C., Spakowitz, A.J., Theriot, J.A., 2010. Bacterial Chromosomal Loci Move Subdiffusively through a Viscoelastic Cytoplasm. Phys. Rev. Lett. 4.

West, S.C., 2003. Molecular views of recombination proteins and their control. Nat. Rev. Mol. Cell Biol. 4, 435–445. https://doi.org/10.1038/nrm1127

Wiktor, J., Gynnå, A.H., Leroy, P., Larsson, J., Coceano, G., Testa, I., Elf, J., 2021. RecA finds homologous DNA by reduced dimensionality search. Nature 597, 426–429. https://doi.org/10.1038/s41586-021-03877-6